BDX-613-1257

HYBRID MICROCIRCUIT INTRACONNECTION PROCESSES

PDO 6984719 and PDO 6984743,
Topical Report

H. B. Bonham, Project Leader

Project Team:
N. T. Panousis
W. A. Piper

Published August 1976

Prepared for the United States Energy Research and Development Administration Under Contract Number E(29-1)-613 USERDA

Bendix Kansas City Division

DISCLAIMER

NOTICE

Printed in the United States of America

Available From the National Technical Information Service, U. S. Department of Commerce, 5285 Port Royal Road, Springfield, Virginia 22161.

Price: Microfiche $2.25
Paper Copy $5.45

BDX-613-1257
Distribution Category UC-38

HYBRID MICROCIRCUIT INTRACONNECTION PROCESSES

Published August 1976

Project Leader:
H. R. Bonham
Department 842

Project Team:
N. T. Panousis
W. A. Piper

PDO 6984719 and
PDO 6984743
Topical Report

Technical Communications

Bendix Kansas City Division

HYBRID MICROCIRCUIT INTRACONNECTION PROCESSES

BDX-613-1257, UNCLASSIFIED Topical Report, Published August 1976

Prepared by A. O. Bendure, D/842, under PDO 6984719

Hybrid intraconnections join thin film networks and applique components into an electrically functional hybrid microcircuit (HMC). Thermocompression (TC) bonding processes were developed to make intraconnections between beam lead devices (BLDs), applique components, such as capacitors and the chromium/gold metallization of the HMC. Thermocompression bonding characterization defined each bonding process in terms of physical process variables. Once a set of machine parameters was correlated to the physical variables for a specific machine, additional machines did not require individual characterization. A set of baseline data was developed which will serve as the reference for subsequent projects in implementing the intraconnection processes into production of HMCs. The processes were developed during a residency of Bendix technical personnel at Sandia Laboratories, Albuquerque, from July 1970 to June 1971.

THE BENDIX CORPORATION
KANSAS CITY DIVISION
P.O. BOX 1159
KANSAS CITY, MISSOURI 64141

A prime contractor for the United States Energy Research and Development Administration
Contract Number E(29-1)-613 USERDA

CONTENTS

ILLUSTRATIONS

TABLES

SUMMARY

Hybrid intraconnections join thin film networks and applique components into an electrically functional HMC. Applique components were intraconnected with thermocompression (TC) bonds to chromium/gold metallized thin film networks. The project determined critical processes, material parameters, quality criteria, and characterization techniques. The work was coordinated by Sandia development program SC-DR-70-514,[1] and then was transferred to Bendix through PDO 6984743.[2]

The program began on July 1, 1970, with a one-year residency of Bendix personnel at Sandia Laboratories, Albuquerque, under the direction of Dr. E. G. Franzak. Initial efforts consisted of organizing the development program and forecasting needed equipment and manpower. The total time schedule was then PERT-charted. Gold beam-lead devices, gold wire, and chromium/gold films had already been selected for these intraconnection technologies.

Thermocompression bonding was developed to provide intraconnections between the HMC gold conductor metallization and gold beam-lead active devices, gold plated external leads, and gold terminated applique devices, such as capacitors. An optimum combination of bonding parameters based on the fundamental physics of the process was developed. This philosophy required bonding equipment to be thoroughly characterized so that the value of bonding parameters (such as force and temperature) indicated on the bonder could be translated into measurable values of the force and temperature within the bond zone.

A gold-to-gold thermocompression (TC) bond requires the application of heat and pressure. Pressure disperses interfacial contaminants and creates a plastic flow which in turn achieves surface conformity and intimate contact. Heat facilitates plastic flow because the ductility of metals increases with increased temperature. Heat similarly facilitates contaminant dispersion because the mobility of surface contaminants is increased. Finally, temperature tends to anneal metals and thus helps to prevent bond rupture after the bond pressure is relaxed. Bond time is important only to the extent that at a given deformation and temperature a minimum bond time is required for bond completion that is much less than the time required for interface temperatures to reach equilibrium. Because the equilibrium of time-to-interface temperature is determined only by the equipment used, bond time does not need to be considered an important process parameter.

A TC bond results when clean metal surfaces are brought into intimate contact over a relatively large percentage of the interfacial area. Under these conditions, a strong solid phase weld may be formed at temperatures well below the melting point of the part.

The K & S Model 573 or 576 Wobble Tool bonder was selected for BL Bonding. The unique Wobble tool rotates and applies pressure to each lead of the beam leaded device (BLD) in rapid succession. This method compensates for variations in lead thickness and substrate camber.

It was established that the cleaning of conventionally packaged BLDs was necessary, that bond time was not a critical parameter, that tool temperature and substrate temperature could be combined to give bond interface temperature, that beam hardness and grain structure were important parameters, and that substrate metallization had to be etched with ceric ammonium nitrate (CAN) before bonding to remove a chromium oxide contaminant.

Samples of four-beam devices (Format 25) were bonded and then visually inspected for bond deformation, bugging height, and other possible bonding defects. Next, the devices were destructively tested by the pull-off test. The failure modes and pull-off strength were recorded. This and other test data were highest when the following criteria were satisfied.

- The mean device pull-off strength was greater than 1 g/mil (0.38N/mm) of beam-width regardless of the failure modes.
- The number of delaminations between the bonded members was less than 0.3 percent of the total number of bonds tested.
- The relative number of bond heel failures was not greater than 25 percent.

In the preceding discussion a bond envelope was derived for Format 25 devices. These symmetric devices had four beams (one on each side) and all four beams were 3 mils (76 μm) wide. When larger devices or devices with asymmetric beam widths were bonded, the pressure at each beam varied as the bonding tool wobbled around the device. Thus, the extrapolation of the Format 25 bond envelope to an envelope for large format sizes was not a simple process.

Reworkability--the ability to remove defective BLDs and replace them with good devices--is an important aspect of hybrid microcircuit (HMC) technology. Five samples of Raytheon three-beam transistors were prepared to determine the bond integrity of the reworked device. The bonding parameters were constant for all samples. The data concluded that two stages of rework would not degrade bond strength.

Bond force, bond time, tool temperature, and substrate temperature were characterized for a RES Model 3000 wire bonder. Bond force calibrations were needed for both the ball and the stitch bonds. Elongation of wire was not a process variable because the bonding operation caused the wire to reach a dead soft state. The bonder had to be set to produce balls less than five wire diameters. Flame-off tip orifice size, wire size and tension, the speed with which the flame cut the wire, the thermal characteristics of the distance from flame to wire, and the bonding tool affected ball size.

A bonding envelope was defined for each combination of metallization: gold bonding pads on HMC, chip capacitor terminations , and chip-on-tab device metallization. Constraints placed on the bond envelope resulted from machine limitations, the occurrence of bond delaminations, and the softening point of the Ablefilm 517 epoxy. Bondability was found to vary from lot-to-lot of chip capacitors.

Fine wire bonds could be removed with the same tool used to remove beam lead bonds. Neither the mean nor minimum strength decreased significantly according to the increased number of times the bond was reworked. It was concluded that a wire bond could be reworked three times by scraping off the old bond and rebonding in the same location.

DISCUSSION

SCOPE AND PURPOSE

Hybrid intraconnections join thin film networks and applique components into an electrically functional HMC. Applique components were intraconnected with thermocompression (TC) bonds to chromium/gold metallized thin film networks. The project determined critical processes, material parameters, quality criteria, and characterization techniques. The work was coordinated by Sandia development program SC-DR-70-514[1] and was then transferred to Bendix through PDO 6984743.[2]

PRIOR WORK

The program began on July 1, 1970, with a one-year residency of Bendix personnel at Sandia Laboratories, Albuquerque under the direction of Dr. E. G. Franzak. Initial efforts consisted of organizing the development program and forecasting needed equipment and manpower. The total time schedule was then PERT-charted. Gold beam-lead, gold wire, and chromium/gold films had already been selected for these intraconnection technologies.

ACTIVITY

The formation of a gold-to-gold TC bond requires the application of heat and pressure. Pressure disperses interfacial contaminants and creates a plastic flow which in turn achieves surface conformity and intimate contact. Heat facilitates plastic flow because the ductility of metals increases with increased temperature. Heat also facilitates contaminant dispersion because the mobility of surface contaminants is increased. Finally, temperature decreases the elasticity of metals. This helps to prevent bond rupture after the bond pressure is relaxed. A minimum bond time is required for bond completion.[3] For typical bonding conditions the time required for bond completion is much less than the time required for interface temperatures to reach equilibrium; therefore, bond time is not an important process parameter.

A TC bond results when clean metal surfaces are brought into intimate contact over a relatively large percentage of the interfacial area. Under this condition, a strong solid phase weld can be formed at temperatures well below the melting point of the parts.

Beam Lead Bonding

Beam lead bonding is a thermocompression bonding technique that simultaneously attaches a component electrically and mechanically to thin film conductors.[4,5] The component is similar to other

semiconductor chips except that the surface metallization does not end at bonding pads on the component itself but extends beyond the edges of the chip in the form of cantilever beams. Hence, it is appropriately called a beam lead device (Figure 1). These leads are able to support the device and to provide electrical connection. Beam lead devices have the following advantages over conventional chip and wire techniques.

- Semiconductor junctions of BLDs are sealed with a silicon nitride encapsulant. This eliminates the necessity of sealing the HMCs that use BLDs.
- Bonding force is applied to the beams only. This prevents fracturing the semiconductor chip during bonding.
- Bonded beams provide a resiliency that prevents temperature stress and mechanical damage during the operational life of the HMC.
- A gold-to-gold bonding system elimates the interaction problems of dissimilar metals, such as gold wire to an aluminum pad.
- All electrical and mechanical connections are bonded in a single automatic operation. This helps to eliminate operator error and reduce manufacturing time.

The disadvantages of BLDs follow.

- There is a limited availability of the BLD.
- The hybrid design lacks flexibility because the lead location is dictated by the device manufacturer.
- The power capability is less than conventional chip and wire devices because a BLD dissipates heat through its leads.

The K & S Model 573 or 576 Wobble tool bonder was selected as the technique to be studied.[6] Temperature and pressure were applied to the bond zone by heating the thin film networks through a work stage and by heating the beams of the device through the bonding tool. The unique Wobble tool rotates and applies pressure to each lead in rapid succession. This method compensates for variations in lead thickness and substrate camber. Figure 2 illustrates the relation of tool, device, and substrate during bonding.

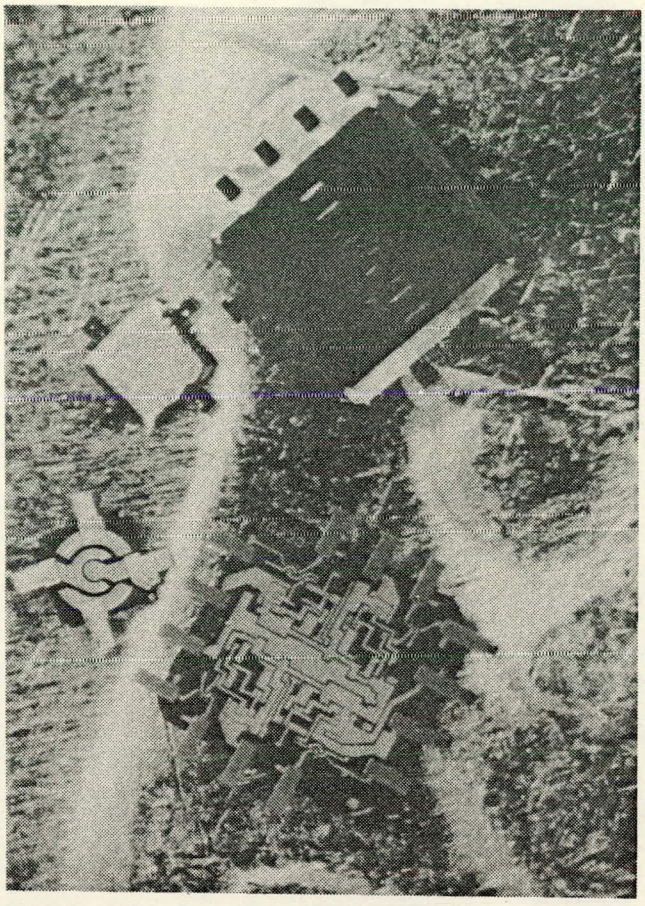

Figure 1. Beam-Lead Device

To begin the bonding operation the chips are placed on a dice dish in a face-down position. The operator then aligns a chip on the dish with the tool. The operator then actuates the bonding head. It descends to a finite distance above the chip. The vacuum system of the tool pulls the chip into the tool cavity. Next the operator aligns the beams with the thin film bonding pattern. Having been properly aligned, the tool descends vertically with the chip to the substrate. After touching the substrate, the bonding tool tilts to one degree off-normal, wobbles twice around the periphery of the chip, rolling over all leads in rapid succession, and then returns to the start position. The process is repeated for each BLD to be attached into the HMC.

Characterization of Parameters

Beam-lead bonding development determined an optimum combination of bonding parameters.[7] Bonding equipment was required to be thoroughly characterized so that the value of bonding parameters, force and temperature, could be translated into measurable values.

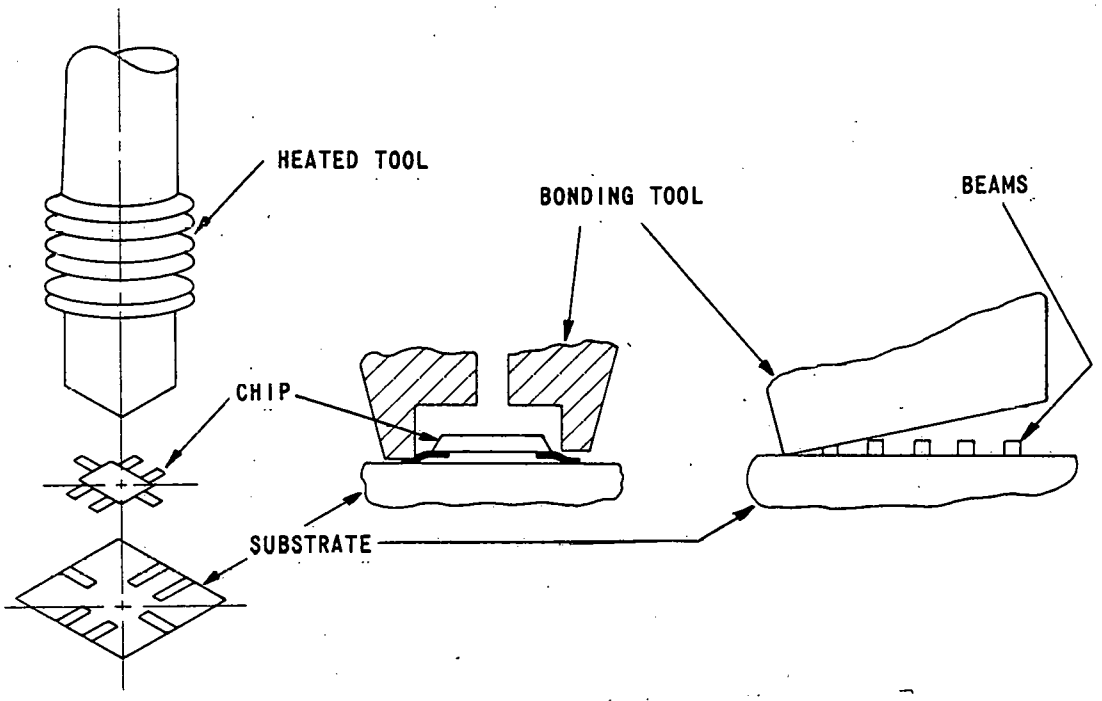

Figure 2. Wobble Bonding

A bonding condition found optimum for the operation of one system could then be used on another system without a great deal of certification data.[8]

Bond force, wobble time, and wobble speed were determined by replacing the substrate holder with a force-to-voltage transducer and cycling the bonder. The output of the transducer (Figure 3). yielded Wobble time and bond force. Because the bonding tool always completed two revolutions, Wobble speed (Sw) in RPM was related to Wobble time (T) in seconds by Sw = 120/T.

Wobble times and force settings are plotted in Figures 4 and 5. Bond force was found dependent on the clearance between the force link and output arm of the tripod assembly (Figure 6). Bond force is essentially constant for force link clearances greater than 0.010 inches (0.254 mm). Therefore any clearance greater than 0.010 inch (0.254 mm) could be used. The bonder manufacturer claims the value of 0.015 inches (0.381 mm) is more likely to yield repeatable forces. Tool and substrate temperatures were characterized with microminiature thermocouples (Figures 7,8,9).

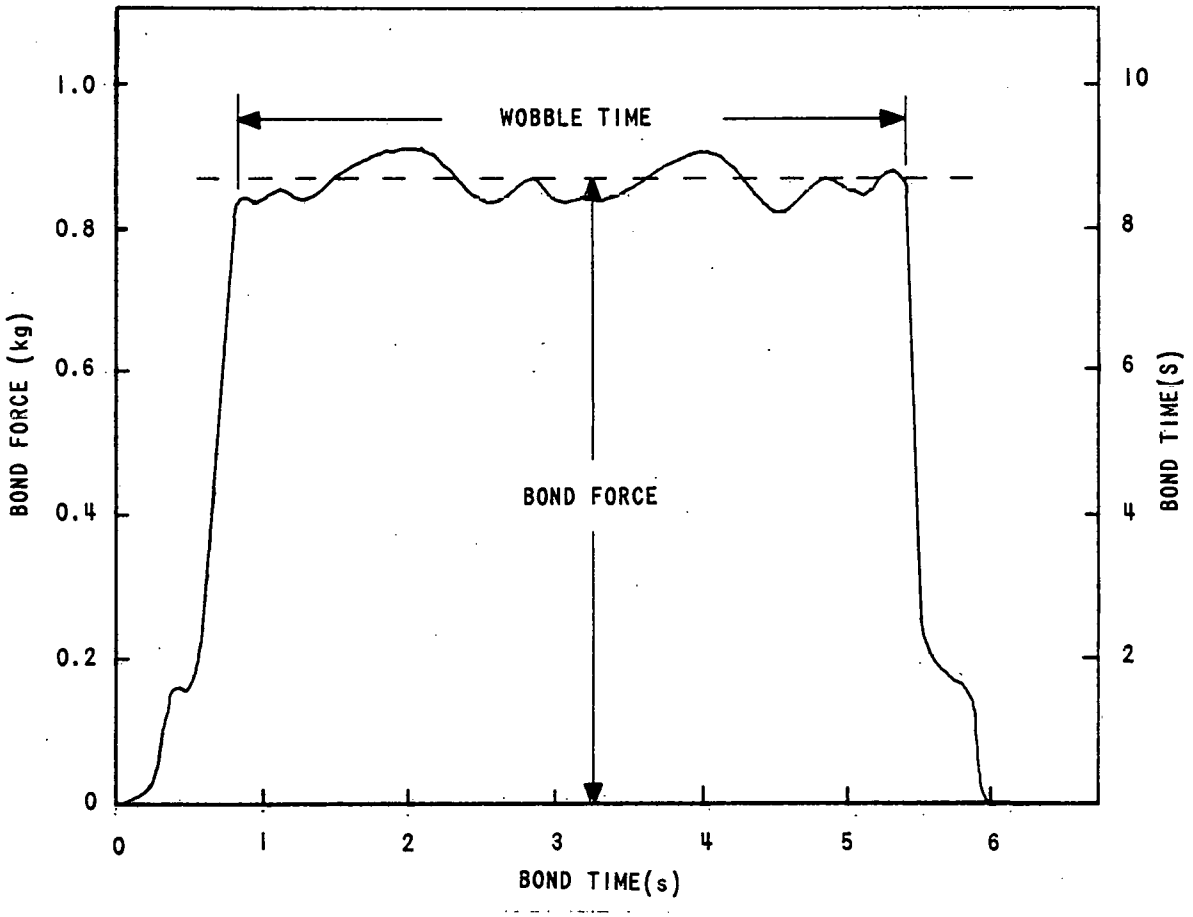

Figure 3. Beam Lead Bonder Wobble Time Calibration

Analysis of Bonding Parameters

Four independent factors of were analyzed: cleanliness, bond time, bond deformation, and interface temperature.

Cleanliness. This is a nonquantitative factor that can only be assessed as "better-than-before" from a bond reliability point of view. Contamination in the interface region determines the amount of mechanical and thermal energy required to achieve a reliable bond

From one lot, 200 uncleaned devices and 200 devices cleaned at Bendix were separately bonded at an interface temperature of 235°C and a bond force of 400 grams (3.92 N). The devices were then pull-tested to destruction (Figure 10). The pull-off strengths and failure modes of each device were recorded (Table 1).

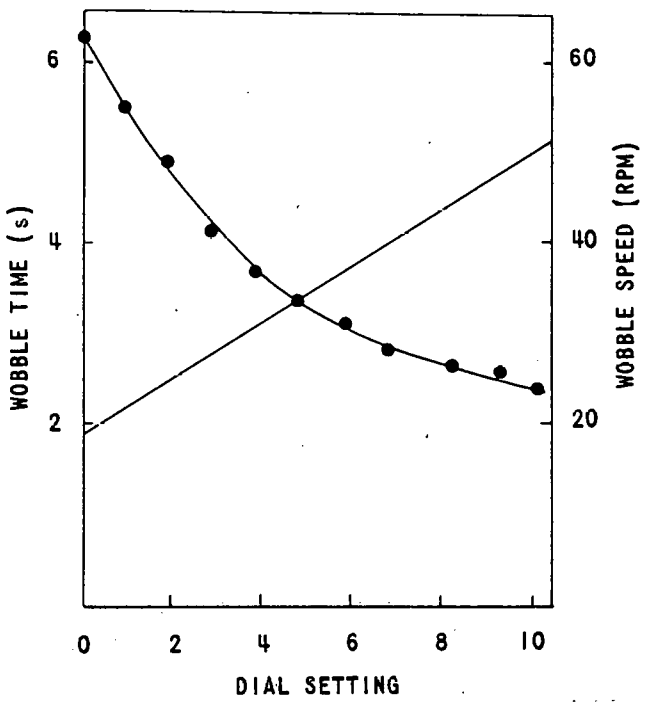

Figure 4. Wobble Calibration

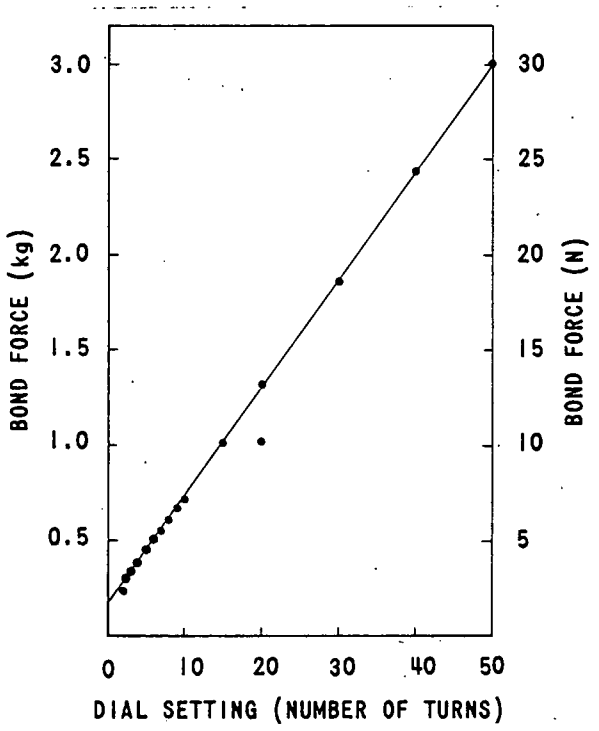

Figure 5. Bond Force Calibration

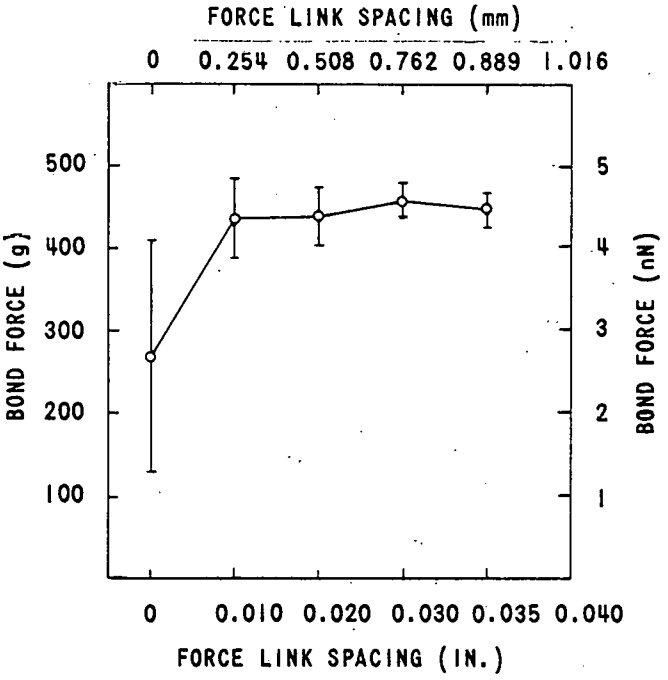

Figure 6. Dependency of Bond Force on Force Spacing

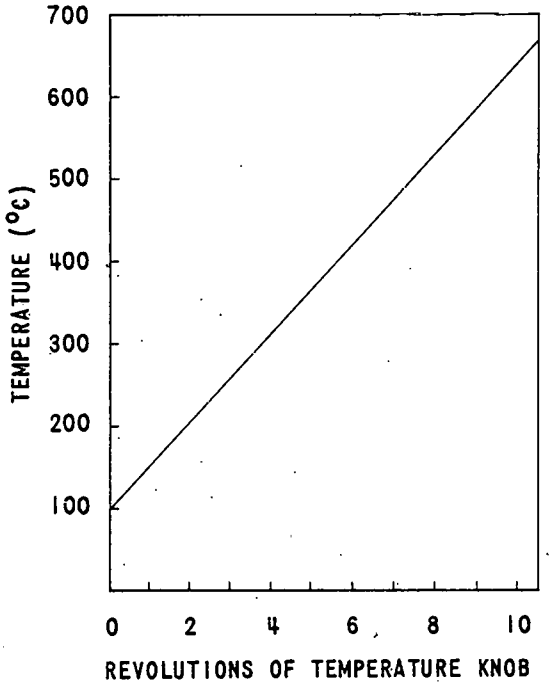

Figure 7. Tool Temperature Calibration

Table 1. Results of BLD Cleanliness on Bondability

Failure mode analysis*	Uncleaned Percentage	Cleaned Percentage
Beam peeling off silicon	36.3	37.8
Beam broken	0.7	0.4
TC bond failure	2.3	0.7
Beam at edge of silicon	25.7	24.3
Beam at heel of bond	35.7	36.8

*Beams measured at 12 g (120 mN) average pull-off strength ($\bar{X}$) with a standard deviation of 4.4 g (44 mN) and 4.2 g (42 mN) (σ) for uncleaned and cleaned devices respectively.

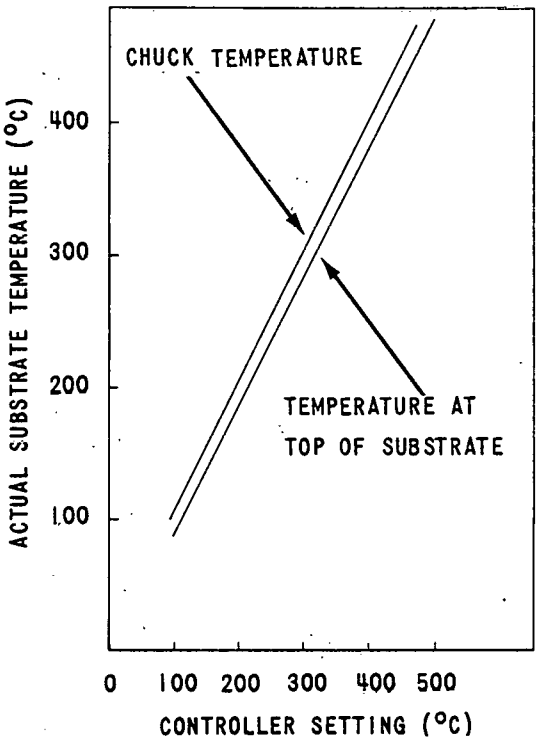

Figure 8. Substrate Temperature Calibration

The mean pull-off strength and standard deviation were essentially the same for both cleaned and uncleaned devices. The only failure mode with a difference between the cleaned and uncleaned samples was the relative number of TC bond failures.

The bond failure rate for uncleaned devices was more than three times the bond failure rate for cleaned devices.

An additional cleaning experiment evaluated cleaned and uncleaned devices which were shipped in an as-etched array. These devices were mounted on a sapphire disk with a holding wax. The pull-off strength and the relative number of TC bond failures were the same for both the cleaned and uncleaned samples. The necessity of cleaning BLDs therefore depends on the packaging used by the device vendor.

Bond Time. Studies have shown that reliable gold-to gold TC bonds can be formed in less than 100 milliseconds.[3]

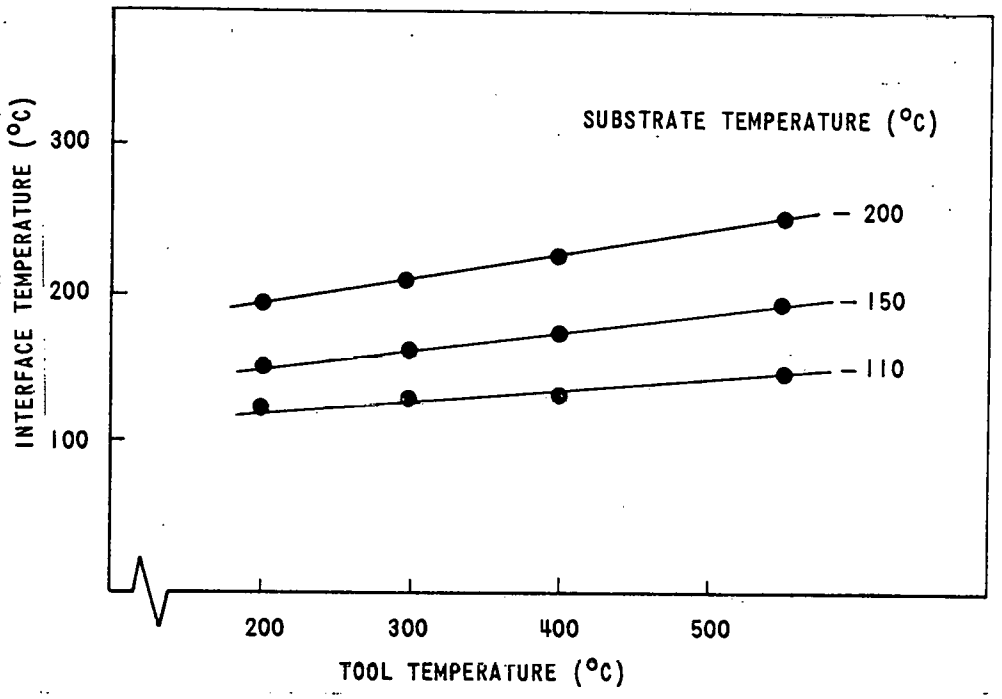

Figure 9. Experimental Interface Temperatures

Wobble speed was calibrated (Figure 4) as a function of dial setting by inserting a force transducer in place of the substrate chuck. The minimum Wobble time was approximately 2.4 seconds. It will be shown later that a time of 0.4 seconds is required to obtain an equilibrium-interface temperature. Therefore, bond integrity did not depend on the Wobble speed setting.

Bond Deformation. This results when pressure is applied to the leads of the device through a heated bonding tool. The allowable deformation can be determined nondestructively by measuring the width of the bond zone and the distance from the bottom of the device to the substrate (bugging). It is a common practice to allow a maximum bugging height of 0.002 inches (51 μm) and a maximum bond width 1.7 times the nominal beam width. From destructive testing, optimum bond deformation can evaluated by the percentage of bond heel and TC bond failures that occur (Figure 11).

During bond schedule development, TC bond failure (D) in excess of 0.3 percent of the total bonds tested indicated insufficient bond deformation and/or interface contamination. Heel failures (F) over of 20 percent indicated excessive bond deformation.

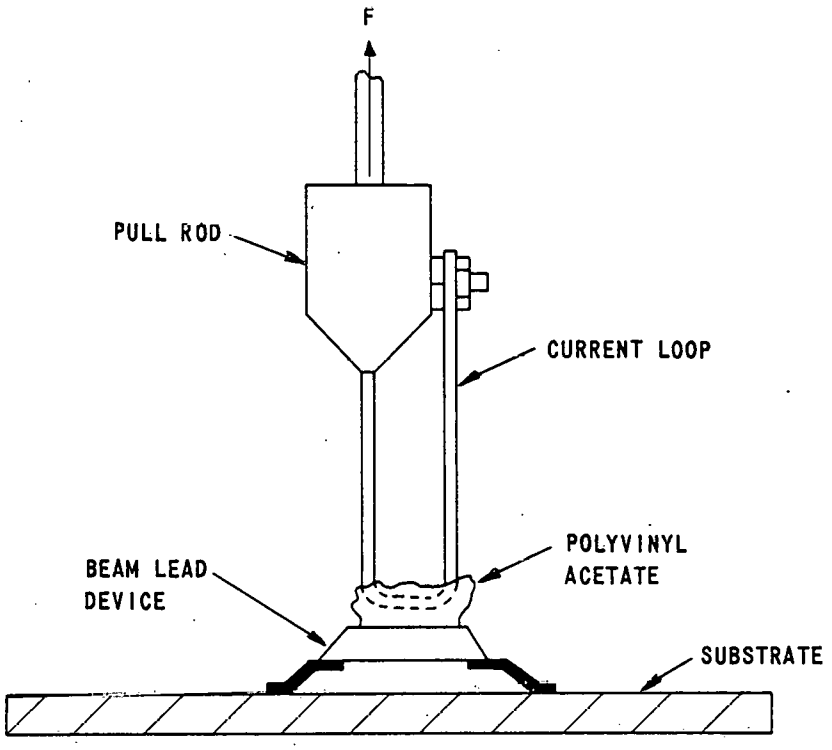

Figure 10. Pull-off Test

Interface Temperature. The bond-interface temperature is determined by the substrate temperature, the bond time, and the bonding tool temperature. The lowest possible substrate temperature prevents degradation of the thin films and other components on the substrate. Therefore, a very high tool temperature is necessary for reliable bonding.

Most beam lead bonding tools are fabricated from tungsten carbide or titanium carbide. If a braze is used to hold the tip or heater in place, the tools are limited to operation below 550°C. Solid tools that do not use a braze can be operated in excess of 600°C, but tool life is short. There is also danger of BLD degradation when the maximum temperature of the chip exceeds 370°C.[8,9] Some protection for the device is obtained by the air flow around the chip caused by the vacuum. Heat transfer analysis was used to calculate the average chip temperature as a function of bonding tool temperature, device size, and configuration.

If the chip reaches a uniform temperature and if negligible heat is lost due to radiation, then the heat flow into the chip from the tool equals the heat flow out of the chip due to convection. Heat flow into the chip depends on thermal contact resistance between the tool and the leads of the tip. Heat flow out of the

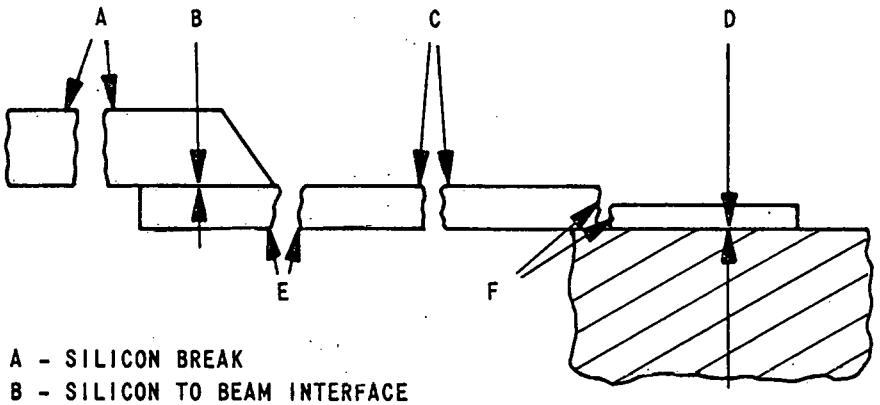

A - SILICON BREAK
B - SILICON TO BEAM INTERFACE
C - BEAM BREAK
D - BOND FAILURE
E - BEAM AT EDGE OF SILICON
F - BEAM AT HEEL OF BOND

Figure 11. Beam Lead Failure Modes

chip depends on the volume and velocity of the air flowing past it. Mr. A. O. Donaldson, Sandia Laboratories, Albuquerque, has determined that at a steady state

$$h\ A\ (T_t - T_c) = h^1\ (T_c - T_a)\ A^1.$$

Where

h is the thermal contact resistance beam to tool, 880 Btu/ft^{2}hr°F (5.88×10^5 $\frac{J}{m2}$ hr°C),

h^1 is the thermal convection resistance, 36 Btu/ft^2 hr°F (2.4×10^5 $\frac{J}{m2}$ hr°C),

A is area of contact beams to tool in square mils

A^1 is the surface area of chips plus exposed beams in square mils,

T_t is tool temperature is °C,

T_c is average chip temperature in °C, and

T_a is air ambient temperature in °C (assumed 25°C).

In Mr. Donaldson's equation the chip temperature is directly proportional to tool temperature, and the proportion depends on chip and beam dimensions. Because the beam dimensions of most BLDs are

standard,* the dimension of these chips can be related to the number of beams they possess. The average chip temperature is a function of the number of beams on the chip (Figure 12). These curves are calculated from the standard device configuration, an air flow rate of 2 cubic feet ($0.057m^3$) per hour around the chip, ambient air temperature (25°C), and a square chip with an equal number of beams on each side. Increasing the number of beams (heat paths) increases the chip temperature. However, when the number of beams increases above four, chip size increases. The

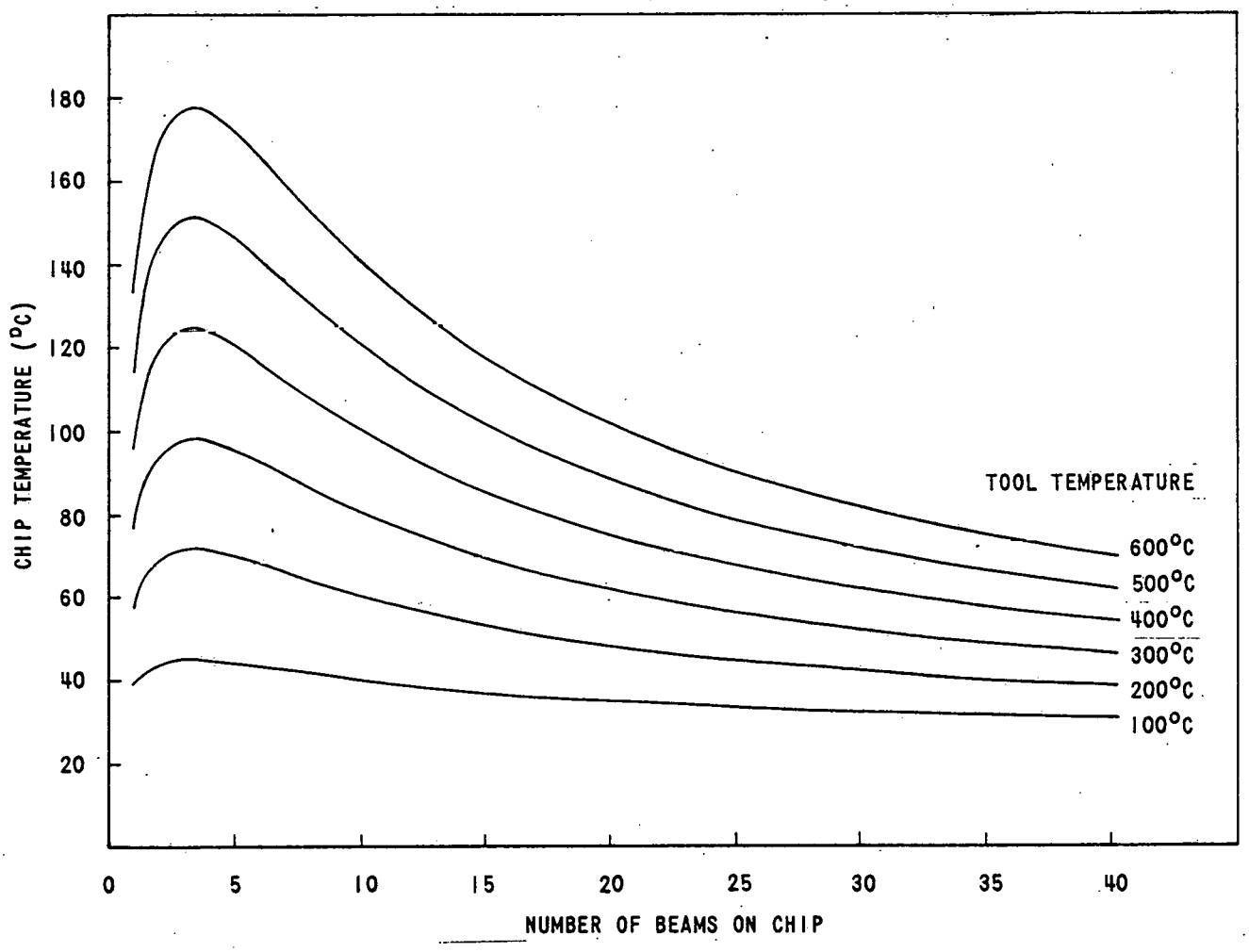

Figure 12. Chip Versus Beams

*Standard beam dimensions are 5 mils (125 μm) long, 0.5 mils (125 μm) thick, and 3 mils (75 μm) wide.

increase in chip cooling by convection now is greater than the increase in heating by the addition of heat paths. Thus, the average temperature of the chip decreases.

For most device configurations and bonding tool temperatures, the 370°C limitation is not to be exceeded; for small devices and high tool temperature, the chip temperature should not approach 370°C.

Heat transfer analysis[9] was used to calculate the temperature at the interface between the beam lead and the substrate. This was a function of time, tool temperature, and substrate temperature. The analysis consisted of using Henning and Parker's solution:

$$\theta\ (F) - 1\ (1 - a)\ e^{a^2 F}\ \text{erfc}\ (a\ F) \qquad (1)$$

where

$$a = \frac{1}{1 + 1/2 \frac{k_t p_t c_t}{k_s p_s c_s}}$$

and

k = thermal conductivity

p = density,

c = heat capacity,

F = Fourier number (= a_s x time/R^2),

a = thermal diffusivity,

R = radius of junction,

$$\theta = \frac{T_I - T_t}{T_s - T_t}, \qquad (2)$$

T = temperature

and subscripts

s = substrate,

t = tool, and

I = Interface.

The constants for the interface temperature achieved during bonding,

k_t = 20 Btu/hr-ft °R (7.03×10^{-4} J/hr-m-°R),

C_t = 0.06 Btu/lb-°R (139 J/kg-°R),

P_t = 976 lb/ft^3 (4.67×10^4 Pa),

k_s = 11.7 Btu/hr-ft°R (4.1×10^4 J/hr-m-°R),

C_s = 0.25 Btu/lb-°R (581 J/k_g-°R) and,

P_s = 250 lb/ft^3 (1.2×10^4 Pa).

These properties and an approximate effective value of R equation (3) yield

a = 0.61,

and F = 17 x (time) where time is in seconds.

Rewriting for Theta, tool, substrate, and interface temperature

$$T_I = A (T_t - T_s) + T_s,$$

Where

$A = 1-\theta$

Thus, interface temperature is a linear combination of tool and substrate temperature. The thermal characterization constant (A) is a function of the thermal and geometric characteristics of the system and of bond time (Figure 13). For bond times greater than 0.4 seconds, the characterization constant is dependent on time. With a characterization constant value of 0.11 the interface temperature is described

$$T_I = 0.11 (T_t - T_s) + T_s$$

or

$$T_I = 0.11 T_t + 0.89 T_s.$$

Interface temperature is more dependent on the substrate temperature than on tool temperature. This is clearly indicated by the coefficients of T_t and T_s in the preceding equation and was anticipated because of the large thermal mass of the substrate holder compared to the thermal mass and thermal conductivity of the bonding

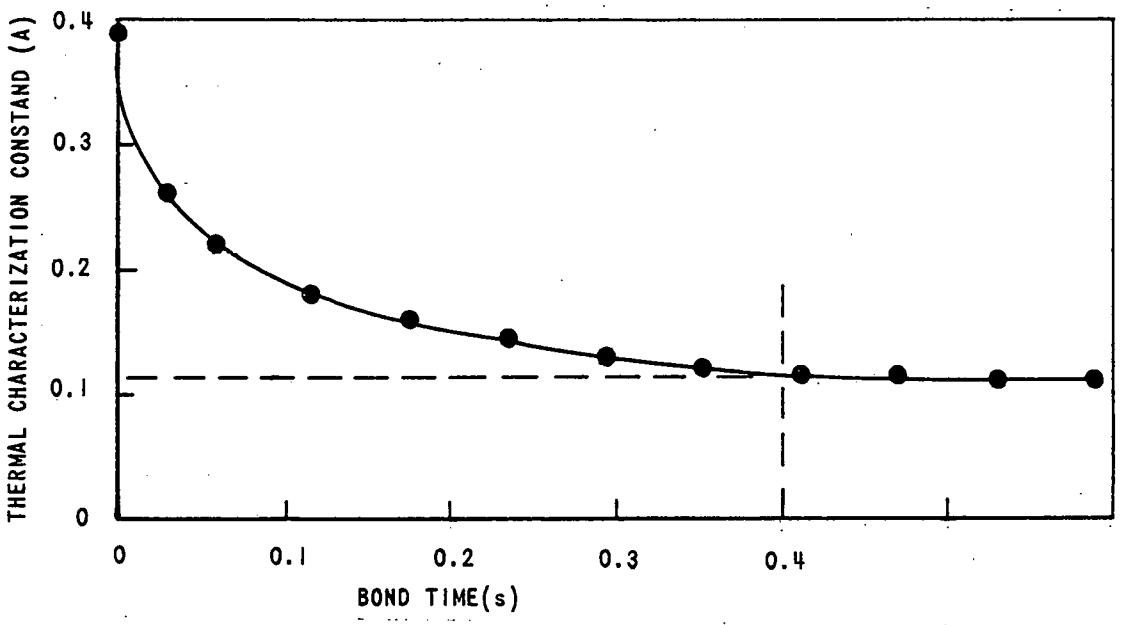

Figure 13. Thermal Characterization Constant Versus Bond Time

tool. The greater dependence on substrate temperature indicates the necessity of maintaining the temperature of the bonding tip as high as practical. This would overcome the heat loss of the cooler substrate.

To verify that the calculated curves were accurate, the actual interface temperatures were measured using evaporated thin film chromel-alumel thermocouples. These thermocouples were calibrated by placing a known temperature gradient across the couples (Figure 14).

A tool temperature controller was built to ensure a constant temperature, ±10°C over the range of 100 to 600°C during the entire bonding cycle. The substrate temperature controller supplied with the bonding machine proved to be quite accurate. Because of the large thermal mass of the substrate holder, this accuracy was more than adequate to ensure a uniform substrate during the bonding cycle.

The interface temperature (Figure 15) was obtained by bonding one lead of a BLD directly on top of the thermocouple junction. The output from the thermocouple was displayed on a chart recorder (Figure 16). An equilibrium-interface temperature was obtained within 0.4 seconds. The interface temperatures were measured at 0.4 seconds to correspond to the time used for the calculated interface temperatures (Figure 15).

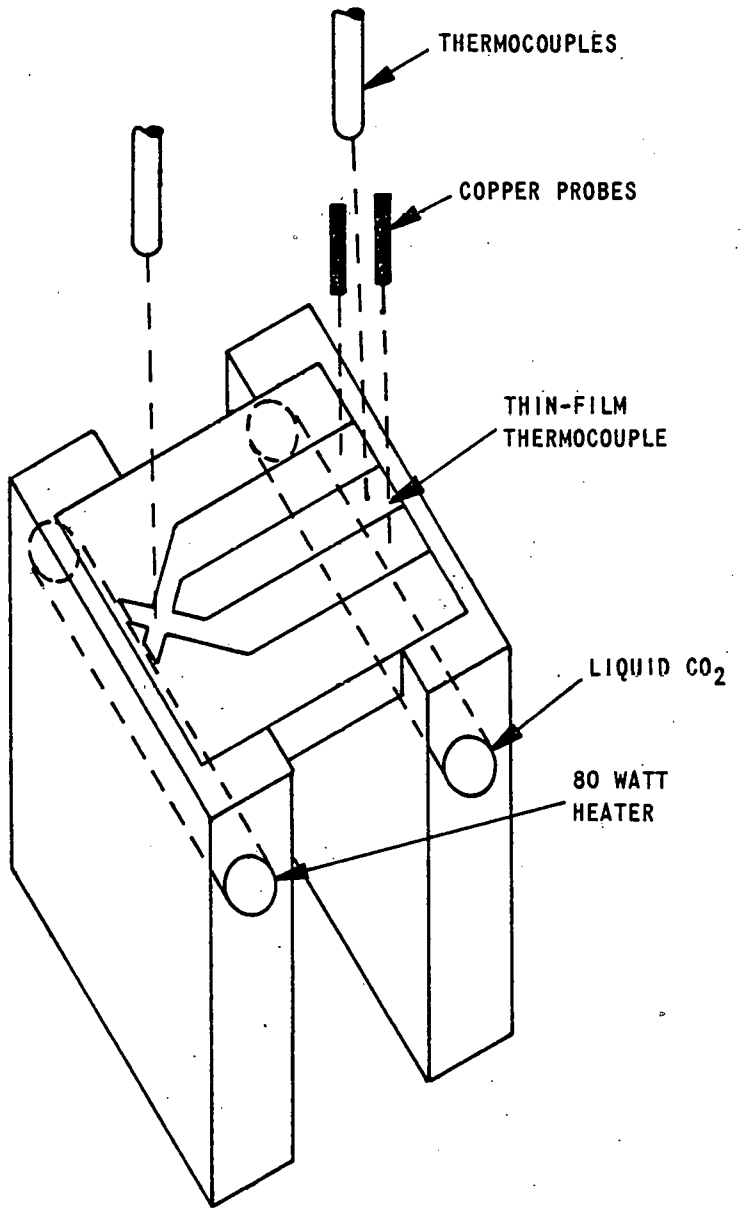

Figure 14. Thin-film Thermocouple Calibration

The measured interface temperatures are within ±5°C of the calculated temperatures. The line which represent the best fit to the experimental points has the equation

$$T_I = 0.11\ T_T + 0.87\ T_S.$$

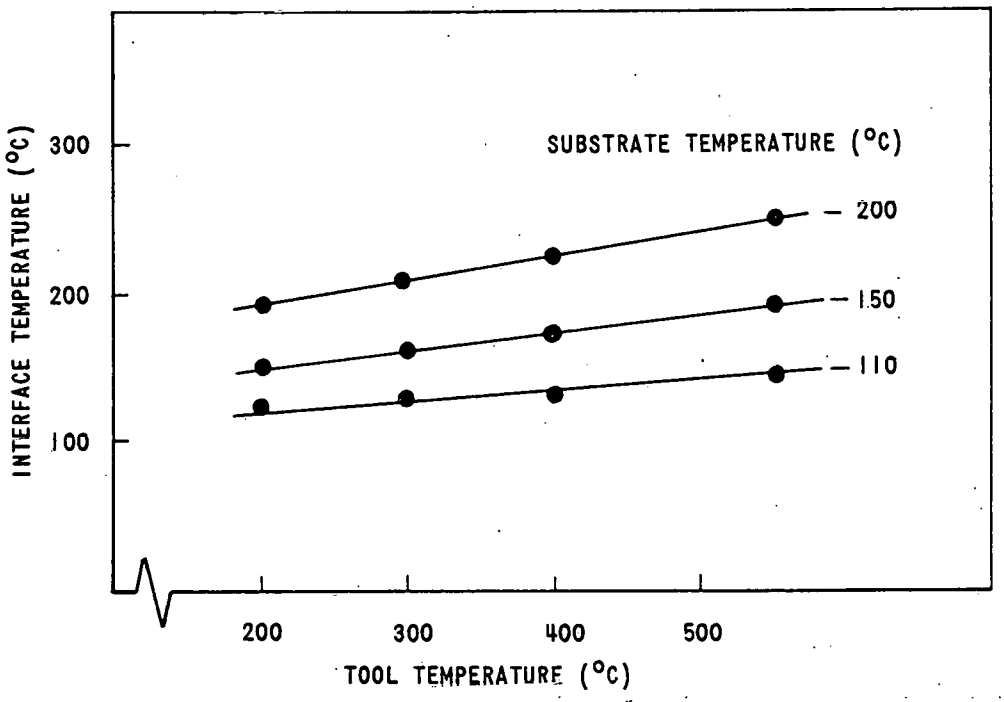

Figure 15. Experimental Interface Temperature

This is in excellent agreement with the calculated equation. Therefore, it is practical to combine the tool and substrate temperatures into the most significant process related temperature--that temperature occurring at the bond interface.

Analysis of Material Parameters

Two additional parameters which affect beam lead bonding are the material characteristics of the beam leads and the bonding-pads properties.

Beam Properties. The leads of BLDs are electroplated gold. Lead dimensions are typically specified by the manufacturer and cannot easily be varied for evaluation. The parameter of most interest is beam hardness. When devices with hard beams were scheduled for development and soft beams were received for production, the production bonds became excessively deformed. Likewise, insufficient deformation results when soft beams were used for schedule development and hard beams were received. To evaluate the influence of beam hardness and to determine optimum beam hardness, Mr. J. R. Adams, Sandia Laboratories, Albuquerque, evaluated 12 wafers of beam lead transistors obtained from

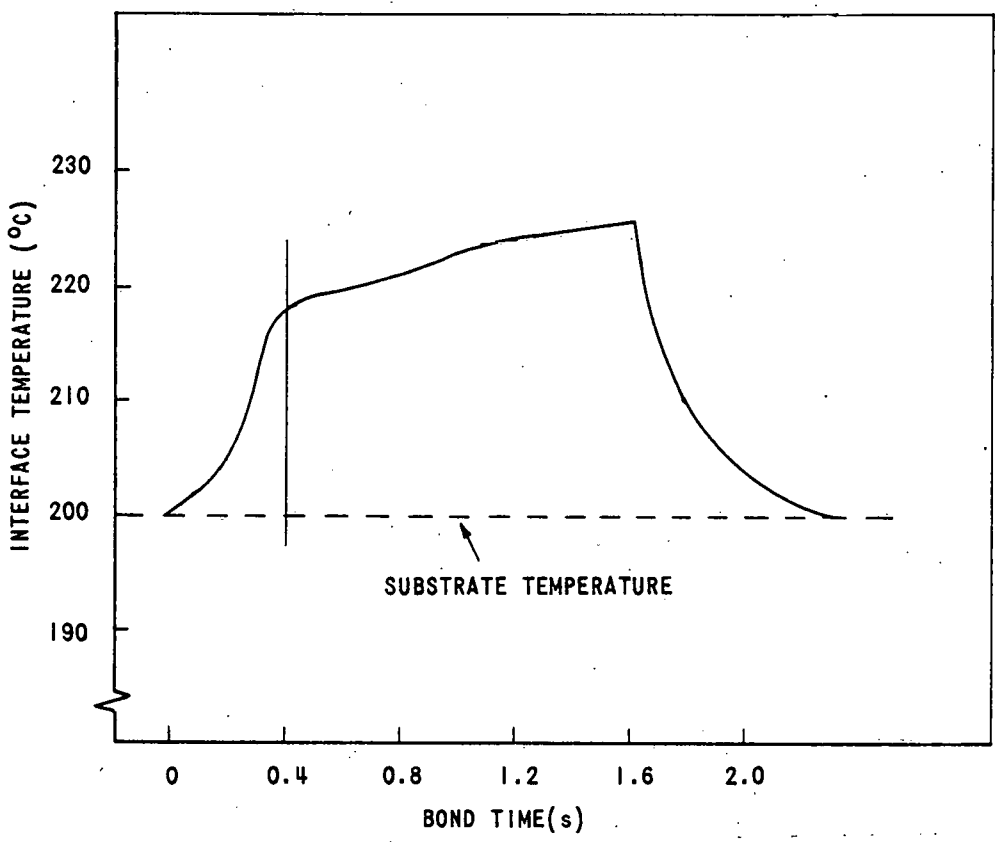

Figure 16. Dependency of Interface Temperature on Time

Raytheon Semiconductor.[10] These wafers were processed through standard device fabrication procedures to the final plating of the beams. The devices were then plated under controlled conditions to yield a range of hardnesses for evaluation.

Hardness of the gold beams on each of the 12 wafers were measured at Raytheon with a Kentroy microhardness tester using a Knoop diamond indenter. They were again measured at Sandia with a Leitz microhardness tester using both Vickers and Knoop indenters. Samples were sent to Bendix Kansas City for measurement with a Zeiss microhardness tester with a Knoop indenter. The force used in every case was 15 grams (0.15 N) except for the Vickers measurements where a 25 gram (0.25 N) force was used.

A sample of devices from each wafer was glued with glycol phythylate face up to an alumina substrate. The leads of the devices were then pulled individually to determine the mechanical strength of the individual leads before bonding. From each of the 12 wafers of beam lead transistors, 120 devices were randomly selected and bonded to 12 substrates.

Finally, the substrates were assembled into kits for Febetron and pull-off testing. Three substrates from each wafer group were selected for pull-off testing and for three levels of Febetron testing. This gave a statistical sample of 30 devices or 90 bonds from each wafer. The substrates intended for Febetron testing were bonded with an industrial epoxy to aluminum discs (anvils) 38 mm diameter by 6 mm thick and cured at 65°C for 20 minutes. The 108 substrates of beam lead transistors selected for Febetron testing were shot at levels of 2, 4, and 8 cal/g Ni. A visual inspection followed. The substrates selected for pull-off testing were 100 percent pull-tested, and the forces were recorded.

Results of the microhardness measurements revealed that as much as 50 percent self-annealing occurs at room temperature over a 15-week period. Further annealing during bonding is caused by higher temperatures. For these reasons the recorded hardness data (Table 2) are those readings closest to the time of testing. These readings vary by less than 5 percent of the last readings.

Table 2. Beam Lead Hardness Data

Wafer Number	Knoop Hardness (kg/mm^2)	Wafer Number	Knoop Hardness (kg/mm^2)
1	75	7	108
2	77	8	116
3	96	9	119
4	102	10	121
5	105	11	122
6	107	12	124

Results of the individual beam pull-strengths revealed little or none of the expected correlation to beam hardness. The average pull-strength of the individual beams was 10.7 grams (0.105 N) which is commensurate with the known cross sectional area of the beam.

The substrates were then visually inspected for obvious defects, such as broken, and/or unbonded beams. No broken or unbonded leads were noticed although there were numerous cracks in the beam next to the silicon and at the heel of the bond.

The device pull-off tests, on the other hand, reveal peaks in the pull-off strengths at two different beam hardnesses (Figure 17) because something besides hardness alone influences the strength of the beams.

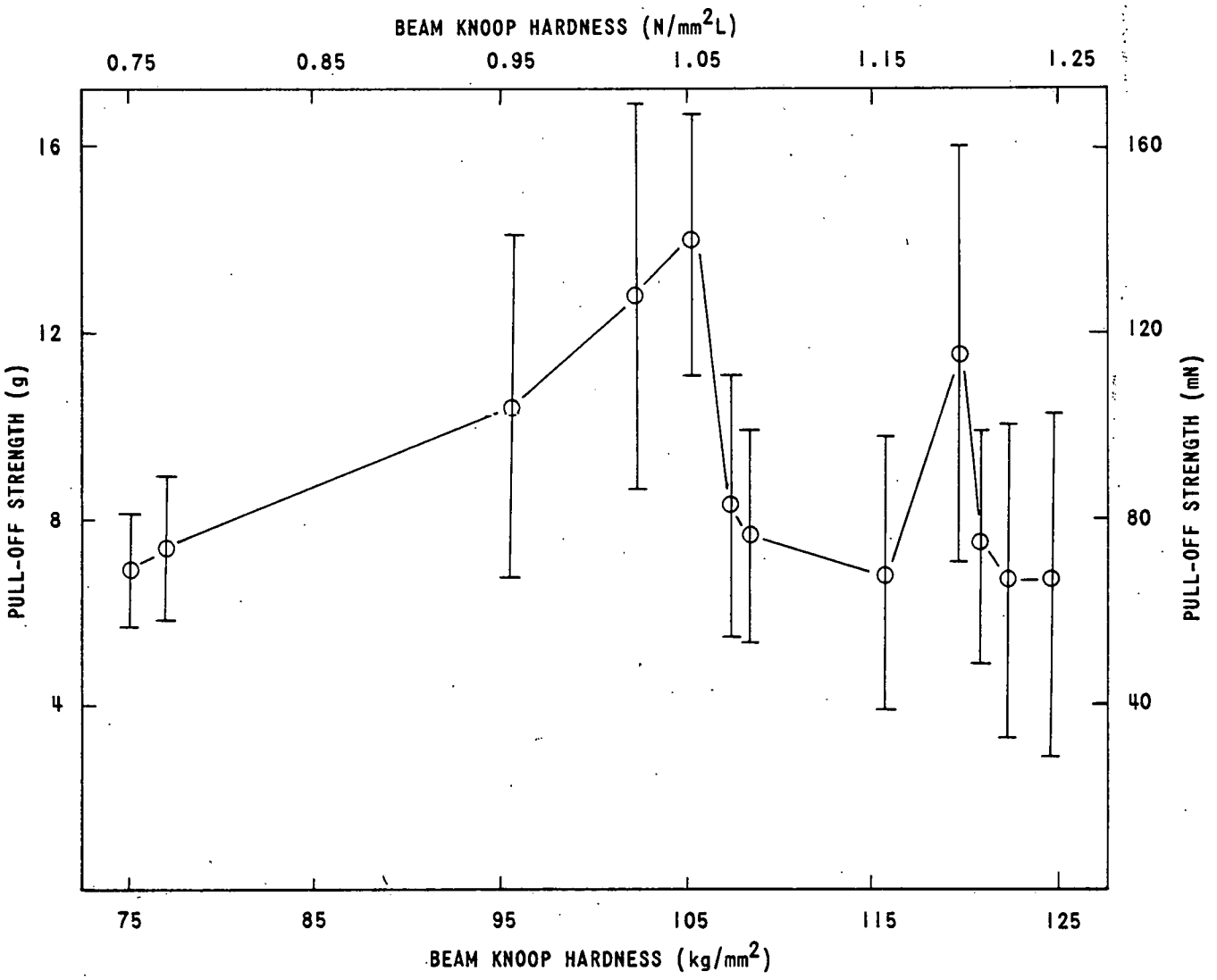

Figure 17. Pull-off Measurements Related to Hardness

Analysis of the failure modes in pull-off testing reveals a sharp reduction in heel failures at the two peak points (Figure 18). The number of remaining failures is equally divided between breaks at the silicon and peeling away from the silicon. A summary of the failure mode analysis for pull-off testing is shown in Table 3.

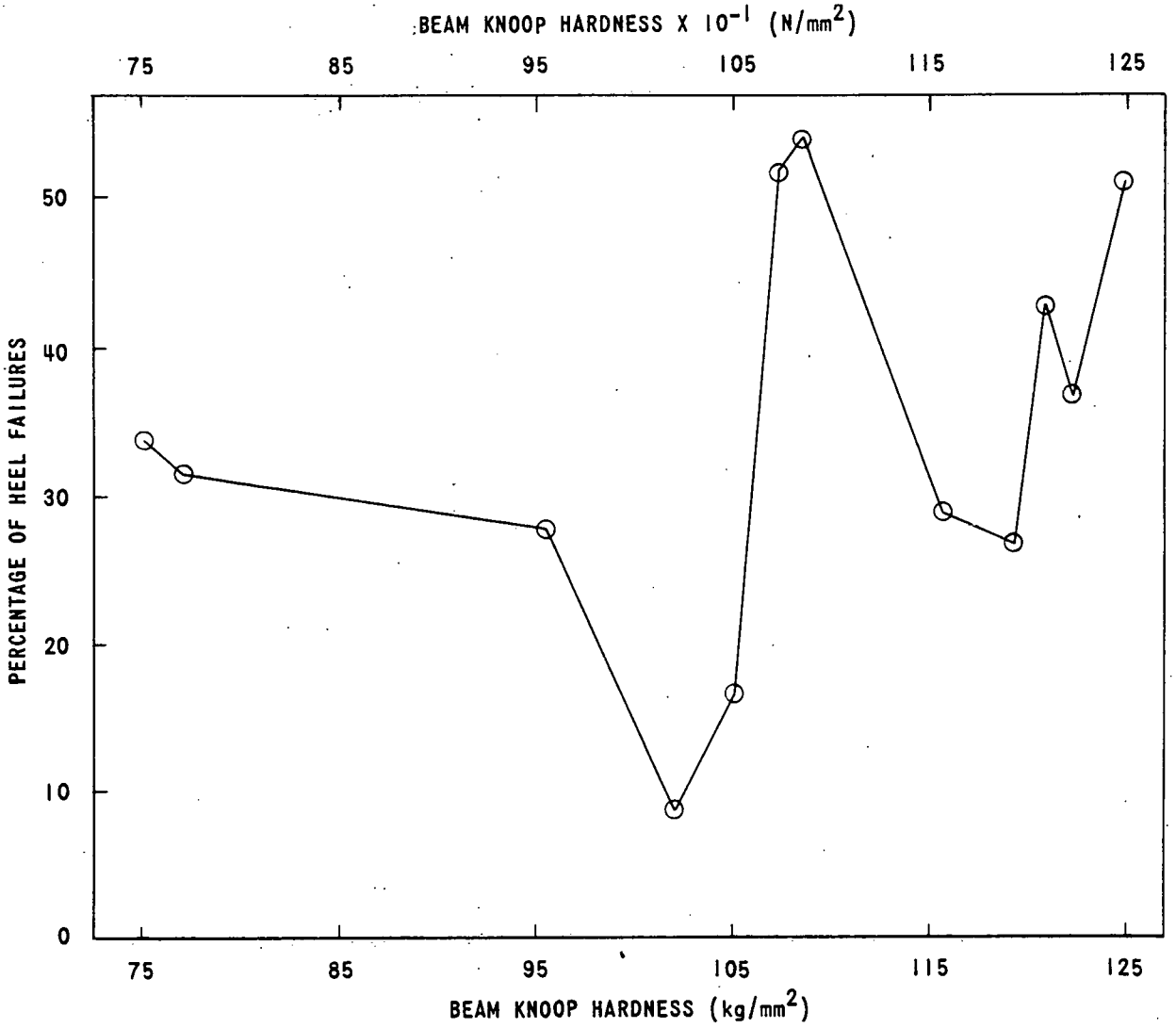

Figure 18. Pull-off Heel Failures Related to Hardness

Every beam that peeled off the silicon occurred on the two-beam side of the device. This was expected because the contact area of the single beam makes an immediate connection to the diffusion contact windows. However, the connection between the two beams and the contact windows are very narrow fingers.

The results of Febetron testing of the 108 beam lead transistors are a function of hardness at the 4 cal/g and 8 cal/g levels (Figure 19). The sharp drop in the percentage of failures that occurs at a hardness of 105 kg/mm^2 corresponds exactly with the maximum in the pull-off strengths (Figure 17). The less pronounced reduction in failures at the 4 cal/g curve and beam

Table 3. Summary of Failure Modes

Failure Mode	Percentage of Total Failures ($\bar{X}$)
Beam peeling away from silicon	30.4
Beam broken at edge of silicon	35.2
Beam broken at heel of bond	24.0
Bond delamination failure	0.4

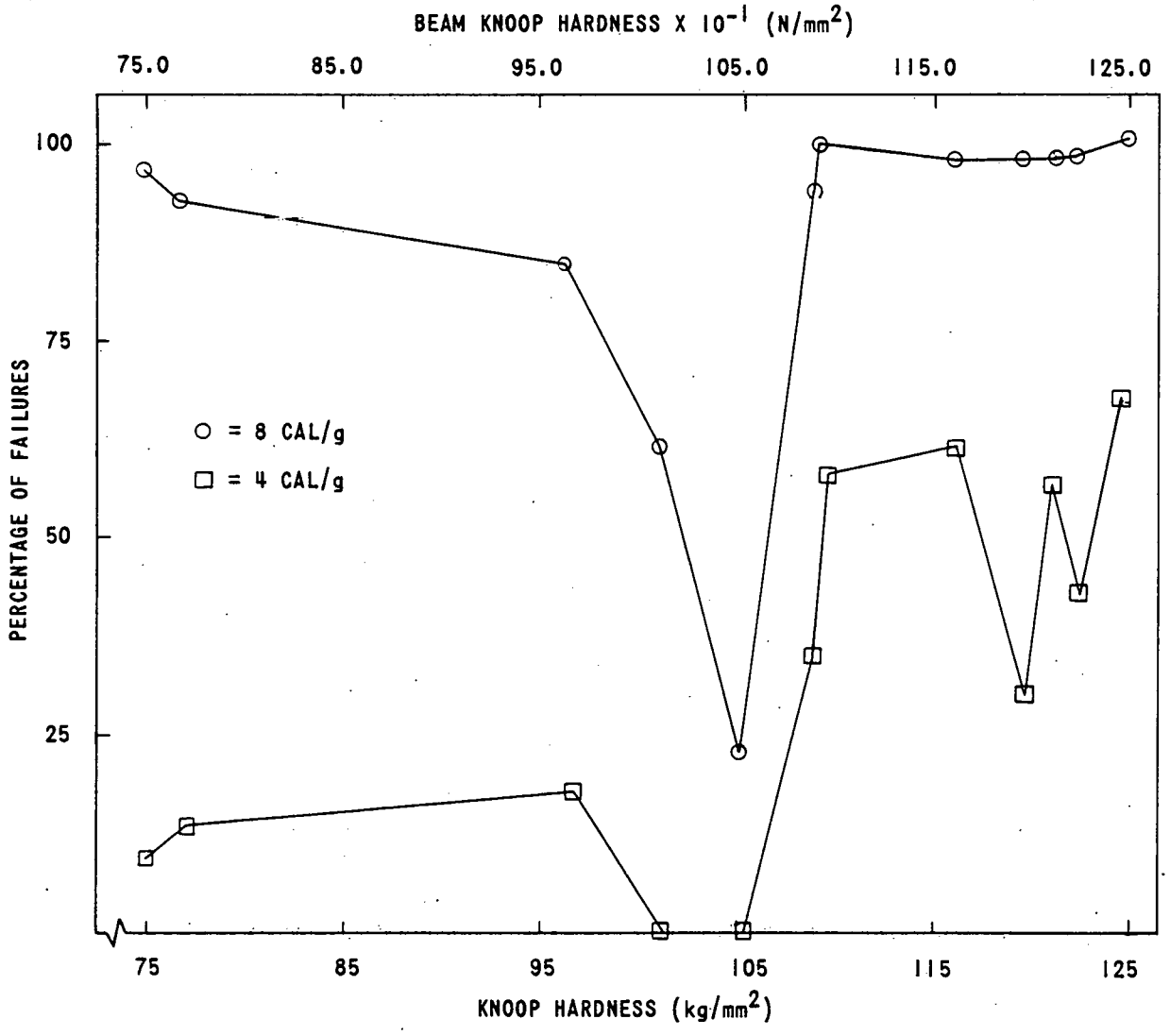

Figure 19. Febetron Failures Related to Hardness

hardness of 119 kg/mm^2 also corresponds exactly with the second peak in the pull-off strengths. This reduction in failures is not apparent at the 8 cal/g level.

Scanning electron micrographs and optical photomicrographs in bright-field and dark-field illumination were taken. These revealed that for hardnesses less than 96 kg/mm^2, the gold plating of the beams was extremely porous but had a fine grain microstructure and a mottled appearance. For hardnesses above 107 kg/mm^2, the beams displayed high porosity, a mottled appearance, and an increased surface grain size. In the hardness range, 96 to 107 kg/mm^2, the grain size is uniform, the color of the beams is more uniform, and there are significantly fewer voids in the gold plate. The sample with a hardness of 105 kg/mm^2 is strikingly more uniform and has more yellow, gold appearance. These investigations conclude therefore that beam hardness is not the only beam qualification criteria and that plating conditions for the gold beams must be carefully investigated. A large majority of the Febetron-tested device failures were beams broken at the edge of the silicon (Table 4). This contrasts the pull-off test where essentially equal failures of the first three types were observed. This can be explained in the following manner.

- Only on the two-beamed side of the device did the beam peel away from the silicon. Because very few of the devices were completely removed from the substrate during Febetron testing, it follows that fewer beams would be peeled from the silicon.

- The majority of failures in Febetron testing were failures of the single lead. Because the heel of the bond has been work-hardened by the bonding operation, it withstands the short duration stresses and flexings imposed by the Febetron shock. However, the area of the beam adjacent to the silicon has not been appreciably work-hardened and is an area of high static concentration. This area experiences rapid flexing during the Febetron shock. It is, therefore, the most vulnerable point.

The 0.1 percent of bond delamination failures shows that the bond schedule was adequate for the entire range of beam hardnesses. Yet this bond delamination failure rate is undesirable for high-reliability hybrid circuits.

Bond Pad. A major interest of bondability is the condition of the bonding pad surface. Surface properties that influence bond integrity are surface finish, absorbed gases, and surface contamination. During TC bonding surface finish is not critical because the metals are subjected to considerable deformation. The interfacial gaps are

Table 4. Febetron Failure Mode Summary

Level	8		4		2	
Beam Failure Mode	A*	B**	A	B	A	B
Peeled from silicon	3	0.7	0	0	3	1.1
Broken at edge of silicon	85	25	96	9	60	1.9
Broken at heel of silicon	12	3.4	4	0.3	34	0.1
Bond delamination	0.3	0.11	0	0	3	0.11

*A-Percentage of device failures
**B-Percentage of total bonds

closed by material flow. The absorbed gases are removed when the parts are heated before bonding. It is very important to remove the interfacial contaminants that would impair adhesion.

Contaminants can be divided into foreign materials and oxide films. Foreign materials (such as particles, greases, salts) can be easily removed by solvent cleaning, but oxides are more difficult to remove. During TC bonding large local forces can fracture and disperse some oxides, but other oxide films must be removed before bonding.

A resistor-conductor network that consisted of layers of tantalum nitride, chromium, and gold deposited respectively on aluminum oxide substrates was studied (Figure 20). The tantalum-nitride resistor network was produced by sputtering tantalum in a nitrogen doped argon atmosphere. Typical sputtering rates of 0.35 nm per second at nitrogen doping levels of 3 percent N_2 (50 mPa) were used to obtain films of 50 nm nominal thickness.

Conductors and bonding pads 3000 nm-thick were prepared by evaporating gold at approximately 3 nm per second. To get satisfactory adhesion of the gold film, a 20 nm layer of chromium was evaporated at approximately 0.5 nm per second on the tantalum nitride film immediately before the gold process. Substrates were preheated to 300°C for the reactive sputtering and to either 200 or 300°C for the chromium and gold evaporation.

Reliable TC bonds can be made to the as-deposited gold pads. However, during fabrication the tantalum-nitride resistor network is stablized by a high temperature air bake (300°C for 2 hours). Following stabilization, reliable TC bonds could not be achieved.[9] The subsequent work involved identifying the mechanism which formed the contaminant, removing the contaminant, and investigating the long term reliability of restored bonds.

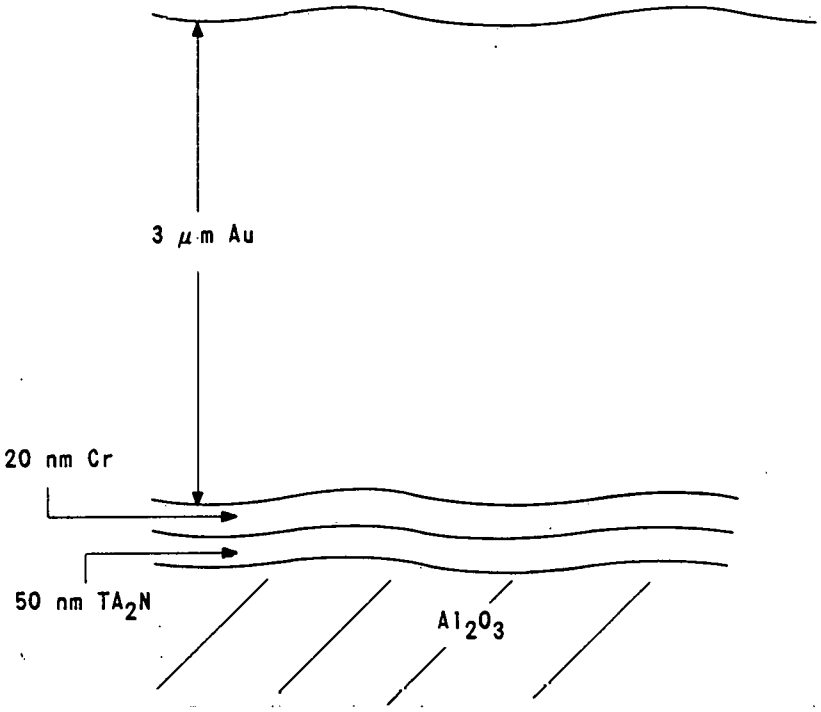

Figure 20. Illustration of the As-deposited Tantalum Nitride-Chromium-Gold Metallization System

Bondability of a gold conductor network was based on an evaluation of gold fine-wire bonds (0.001 inch diameter) and gold plated lead frame bonds (0.127 mm by 0.38 mm in cross section). To evaluate fine wires, 20 consecutive TC bonds were tested. Ball bonds were pulled to destruction in tension. When all the bonds failed as wire failures, the network was defined as bondable. The network was defined as nonbonable when a single bond failed as a delamination or fracture between the gold network and the ball. When if a bond failed in any other manner, it was considered a no-test, and an additional bond was pulled.

Lead frame bondability was based on the failure mode and strength of 19 lead frames. After being TC bonded with a 0.010 inch (0.25 mm) wide tool, they were then pulled to destruction in a 90° peel test. When the bonds had an average strength of 1.00 pound (4.4 N) with a minimum of 0.75 pound, (3.3 N) the network was defined as bondable. When if a single bond delaminated with a strength of less than 0.75 pound, (3.3 N) the network was not bondable. Other than this delamination was considered a no-test, and an additional lead was pulled. A beam lead criterion was not used because the pull-off test does not yield single lead data.

The diffusion of chromium through gold films has been well documented.[12-16] This diffusion was accepted as the mechanism through which bonding is degraded. Resistor-conductor networks were stablized in air for 2 hours at temperatures between 225 to 400°C. The bonding pads were then analyzed for chromium by using the energy dispersive X-ray analysis (Edax), Auger electron spectroscopy (AES), and ion scattering spectroscopy (ISS). Pads were next evaluated for bondability. Table 5 summarizes the results and points to three principal observations. First, there is a direct influence of chromium on the unreliable TC bonds. Second, wire bonding is more sensitive to the contaminant at this lower bonding temperature. Third, the present stabilization cycle for the resistor network, 300°C for 2 hours in air, is in the transition region, a region generally considered unreliable for TC bonding.

The identity of the bonding contaminant was further established by use of electron spectroscopy for chemical analysis (ESCA). Examination of a nonbondable gold film by ESCA definitely established the presence of a chromium oxide on the bonding surface although the lack of standards precluded the identification of the exact oxidation state. The ESCA conclusion was consistent with the inference that could be made from the Auger spectra. Therefore, the diffusion and oxidation of chromium on the surface of the bonding pads were concluded to be the mechanisms through which bonding was degraded.

In the preceding example, the bonding contaminant was not removed by typical solvent cleaning. Therefore, chemical cleaning had to be evaluated. A gold etchant,* potassium iodide-iodine (KI/I_2), and chromium or chromium oxide etchant,** ceric ammonium nitrate (CAN) were studied. In the first set of experiments, the gold etchant was considered. Substrates which exhibited poor bondability and were known to have chromium oxide on the surfaces as a result of resistor stabilization were given a prebond gold etch with the KI/I_2. This removed approximately 200 nm of gold as well as surface contaminants. After the prebond etch, TC bondability was restored. Analysis of the gold bond pads showed that not all the chromium had been removed. The local bonding forces were now sufficient to disperse the remaining contaminant and produce a bond.

---

*The Au etchant is made from 63.46 grams I_2, 100 grams KI in 500 ml deionized H_2O.

**The Cr etchant is made from 164 grams ceric ammonium nitrate dissolved in 200 ml deionized water, 130 ml concentrated nitric acid and diluted to 1 liter with deionized water.

Table 5. Correlation of Bondability to Chromium

Stabilization Temperature (°C)	Bondability		Chromium Detected
	Wire	Lead Frames	
225	Yes	Yes	No
250	Marginal	Yes	No
300	No	Marginal	Marginal
350	No	No	Yes
375	No	No	Yes
400	No	No	Yes

The KI/I_2 etch does not chemically attack the chromium oxide but rather attacks the gold and removes the chromium oxide by undercutting. The KI/I_2 etchant used in a prebond treatment was analyzed for chromium by atomic absorption spectroscopy (AAS). No chromium was found. For detection by AAS, the chromium must be a solution, not a suspended particulate. The failure to detect chromium in the preceding conditions supports KI/I_2 as the undercutting mechanism.

Although the gold prebond etch did restore bondability, it did not completely remove the chromium from the gold bonding surfaces. In addition, the electrical resistivity of the gold conductor network increased as a result of this process. Therefore, an etchant specific to chromium and chromium oxide, CAN, was evaluated. The experiment consisted of submitting resistor-conductor networks to three different treatments. The first group was as-fabricated (not stabilized); the second group was stabilized in air for 2 hour at 300°C but was not prebond etched; the third group was stabilized and then prebond etched with CAN for times ranging between 10 minutes and 16 hours (overnight). The lead frame, fine wire bonds, and surface were then analyzed (Table 6). As before, a correlation was evident between the presence of chromium and the inability to make reliable TC bonds.

The CAN etch chemically attacks the chromium oxide and dissolves it. Thus, it was possible to use AAS to analyze these etchants for the amount of chromium (Figure 21). The extent of the chromium undercutting was measured in the three sample groups (Table 6). The undercutting results are consistent with AAS results for chromium content. Neither shows a correlation with the time of prebond etching.

First order approximations were used to construct a model for the chromium concentration within the gold conductor film. The model

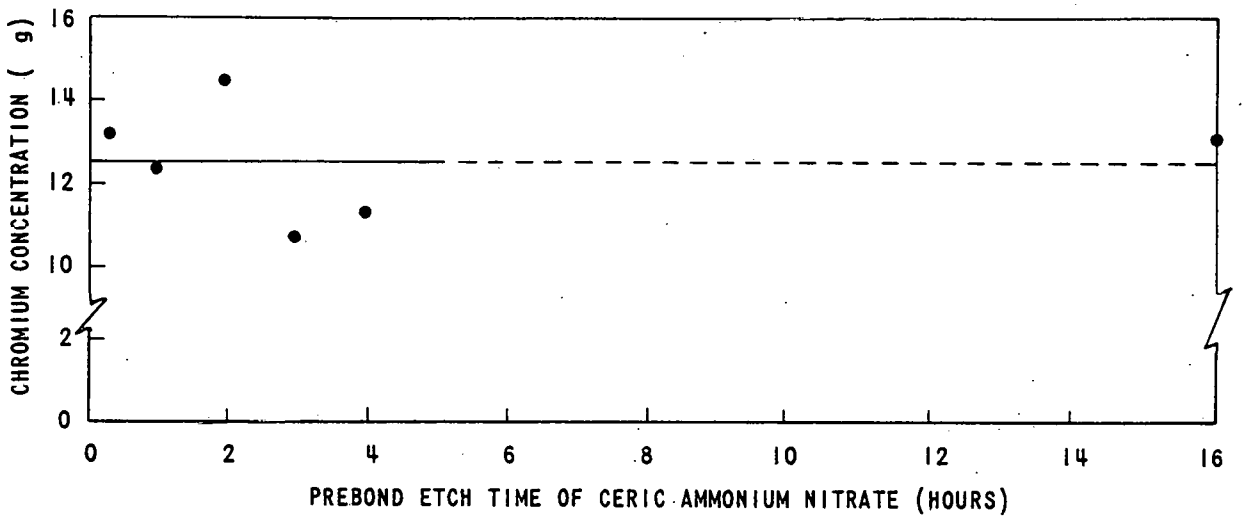

Figure 21. Relation Between Time of CAN Etch to Amount of Chromium Removed

assumed that a chromium thickness could be calculated as the ratio of the weight of chromium to the product of the network area and the density of chromium. In addition, the model considered only the diffusion of the chromium within the gold films. Specifically excluded were any interactions with the tantalum-nitride resistor network or the aluminum-oxide substrate. Details of this profile reflect the particular combination of the preceding processing parameters.

A chromium cencentration profile was determined for a 26 mm by 26 mm network stabilized in air at 300°C for 2 hours. The units were chosen so that the area under the curve is equal to the total amount of chromium (Figure 22). The analysis used to construct the concentration profile follows. Auger electron spectroscopy and ISS were used in a insitu sputter through the chromium oxide layer. The Auger technique indicated that the chromium oxide was dispered in the top 200 nm of the gold film; ISS indicated a depth of 50 nm. Atomic absorption spectroscopy determined that from a total of 135 µg of chromium, 12.6 µg were dispersed in the upper 50 to 200 nm of the gold film (Figure 21) 25.3 µg of chromium were at the original location and 97.1 µg were dispersed in the bulk of the gold film.

Because chemical etching only removes chromium oxide from a bond pad surface, restored resistor-conductor networks can experience additional contamination during circuit operation. Bond pad contamination can degrade bond integrity. To determine the influence of continued chromium diffusion on bond integrity,

restored-film bonds were exposed to high temperature storage, temperature cycling, temperature storage at underrated power, and storage at 75°C with 100 percent relative humidity (Table 7). Neither fine wire nor lead frame bonds degraded. Although not listed in the table, bond integrity was evaluated periodically by pull-testing throughout the duration of each test condition. The periodic pull-strengths were equivalent to the strength before environmental stressing.

A second reliability consideration is the possible loss of adhesion between the gold conductor network and the tantalum nitride resistor network. Research should determine whether CAN prebond etch treatment removes the chromium from between the gold and the tantalum nitride. In this way the treatment could induce delamination of the resistor-conductor network.

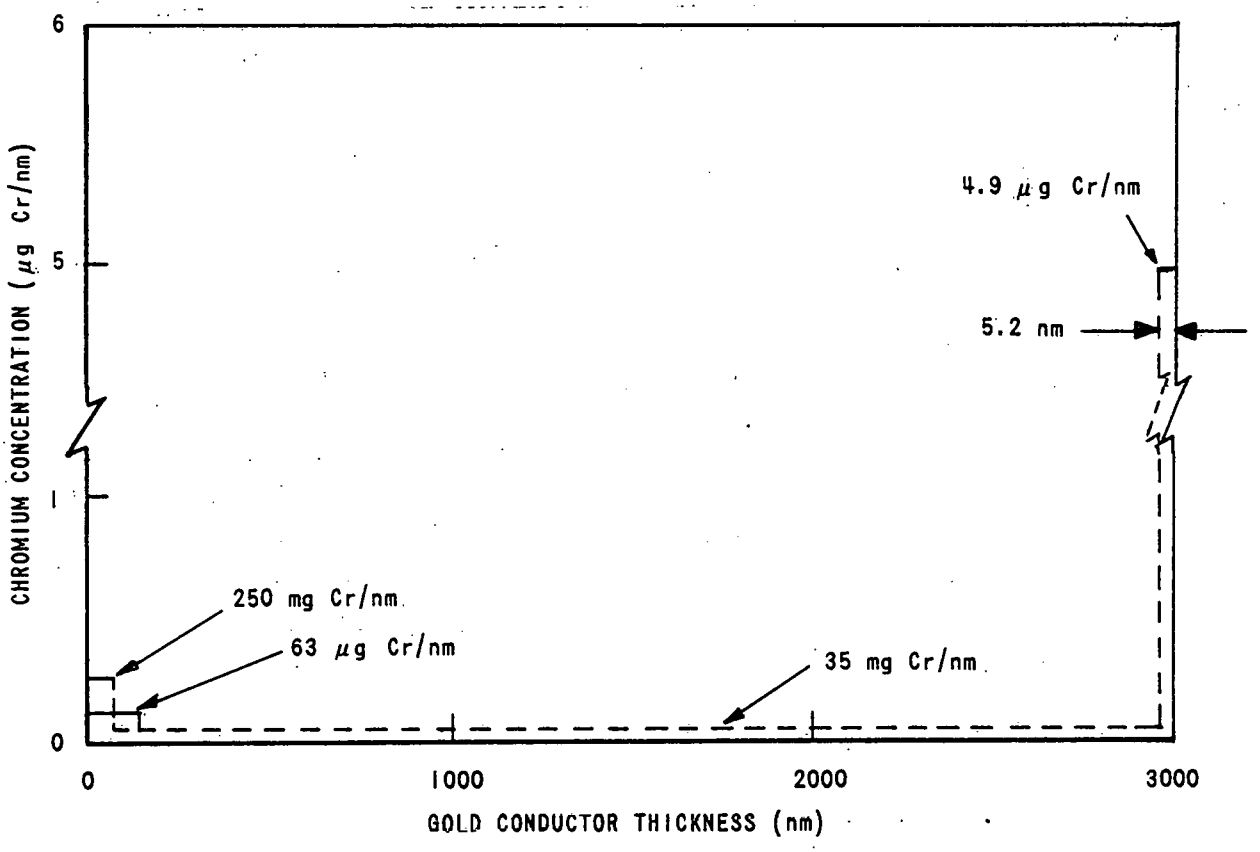

Figure 22. Chromium Concentration Profile

The undercutting measurements (Table 6) and the chromium concentration profile (Figure 22) establish that chromium is present between the gold and tantalum nitride films following CAN prebond

Table 6. Restoration of TC Bondability with CAN Prebond Etch

Sample Condition	Bondability		Chromium on Gold Bonding Surface	Chromium Undercutting on Original Gold Path 5 mils (127 μm) Width
	Fine Wire	Lead Frame		
As-fabricated network	Yes	Yes	No	0.21
Network stabilized in air for 2 hours at 300°C	No	No	Yes	0.68
Network stabilized in air for 2 hours at 300°C then prebond etched in CAN for 10 minutes	Yes	Yes	No	
1 hour	Yes	Yes	No	0.40
2 hours	Yes	Yes	No	0.80
3 hours	Yes	Yes	No	0.31
16 hours	Yes	Yes	No	0.52

etching. In addition, no cases of network delamination were observed in the pull-test of wire and lead frame bonds. The CAN restored networks (Tables 5, 6) passed the conventional tape test for adhesion. As an extreme overtest, networks were given a 96 hour prebond etch treatment with CAN followed by fine wire and lead frame bonding (Table 7). Once again network delamination was not observed in the destructive pull-tests. Therefore, network adhesion was not degraded, and it would not classify as the weakest member in the TC bond.

Three principal conclusions were drawn from this study of the TC bondability of the tantalum nitride-chromium-gold metallization system. First, the diffusion and oxidation of chromium result from a 300°C, 2 hour air bake used to stabilize the tantalum-nitride-resistor network. Several analytical techniques, AES ISS, AAS, and ESCA were used to establish the mechanism through which bondability was degraded.

Table 7. Bond Integrity Versus Environmental Testing

Test	Description	Bondability	
		Wire	Lead Frame
Temp storage	250°C/400 hours in air	Yes*	--
Temp cycling	100 cycles; -50 to +90°C at 150°C/minute	Yes	Yes
Power burn-in	96 hours at 110°C under rated power dissipation	Yes	Yes
Humidity	75°C at 100 percent relative humidity for 96 hrs.	--	Yes

*Restored via KI/I_2 prebond etch

Second, TC bondability of the gold conductor networks could be restored. The contaminant was chemically removed with either KI/I_2 or CAN prebond etch treatment. The KI/I_2 prebond etch treatment left chromium oxide on the gold bonding surfaces while CAN prebond etching completely removed the chromium oxide from the bonding surfaces.

Third, the integrity of bonds made to restored films was not degraded. The tests included storage in air at temperatures up

to 350°C for 200 hours, power burn-in at rated power, temperature cycling 100 times between -50°C to +90°C and 100 percent humidity tests at +75°C. In addition, network delamination at the gold-chromium interface could not be induced by extended etching in CAN for up to 96 hours.

Bond Schedule Development

To this point it has been concluded that cleaning of conventionally packaged BLDs is necessary, that bond time is not a critical parameter, that tool temperature and substrate temperature can be combined to give bond interface temperature,[7] that beam hardness and grain structure are important parameters,[10] and that substrate metallization must be etched before bonding to remove a chromium oxide contaminates.[11] What remains is to establish the effect of bond pressure on bond integrity as a function of interface temperature.

The dependency of bond force to interface temperature was determined by bonding cleaned samples of Format 25 devices at various combinations of temperature and pressure. The Format 25 device was used because its beam configuration is symmetric and simple. This device has only one beam on each side, and the thickness, width, and length of each beam are identical for all beams. The advantage of this geometry is that each beam has the same bonding force during Wobble bonding. Twenty devices were bonded at each point in a matrix of interface temperatures varying from 140 to 235°C in 10°C increments. Bond force varied from 200 to 1000 g (1.96 to 9.6 N) in 50 g (0.49 N) increments. Substrate temperature was limited to 200°C. This prevented further chromium diffusion and prevented thin-film resistor drift. Tool temperature was limited to 550°C to prolong tool life. The maximum usable interface temperature was 235°C.

All devices were visually inspected after bonding for percentage of bond deformation, bugging height, and possible bonding defects. The devices were then destructively tested by the pull-off test. The failure modes and pull-off strengths were then recorded with the bonding parameter combination used. Analysis of this and other pull-off test data showed that the mechanical integrity of the bonded devices were maximized when all the following criteria were satisfied.

- The mean device pull-off strength was greater than 0.39 N/mm of beam-width, regardless of the failure modes which occurred.
- The number of TC bond failures was less than 0.3 percent of the the total number of bonds tested.
- The relative number of bond heel failures was not greater than 25 percent.

A region in the bond pressure-interface temperature plane was established so that bonded devices would meet all the preceding criteria. In the area to the left and below line AEDC (Figure 23), the number of TC failures exceeded 0.3 percent, and/or the mean pull-off strength did not meet the minimum criteria. This line defines minimum bond conditions. In the area above line AB, beams are excessively deformed. Over 25 percent of the heel failures occur and/or pull-off strengths do not meet minimum criteria. This line, therefore, defines maximum bond conditions. Line BC is a process limitation that is the maximum interface temperature. Thus, substrate temperature is not to exceed 200°C, and tool temperature is not to exceed 550°C.

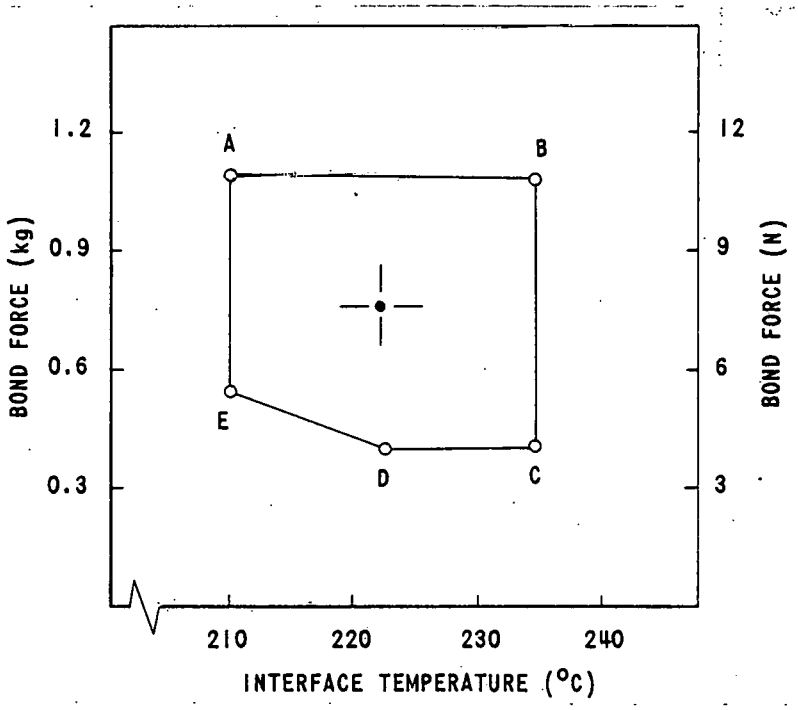

Figure 23. Format 25 Bond Envelope

An optimum point is chosen within the envelope so that the effect of parameter variations is minimized. The point chosen must be sufficiently distant from the boundaries of the envelope so that variations in bond force and interface temperature cannot permit the machine to operate outside the envelope.

Figure 24 illustrates the distribution of pull-off strength of Format 25 device bonded at the optimum bonding point. The distribution is plotted so that the mode of failure is noted.

- Failure B occurred at the interface of the beam to the body of the device; B failures indicate that the weakest point in the system is device oriented and is independent of bonding.

- Failure F is located at the heel of the bond; it is the result of a deformation that weakens the beam at the heel of the bond.

The average strength of the sample exceeds the minimum requirement of 0.39 N per mm of beam width (0.12 N). F failures did not exceed 25 percent. The figure also shows that failures that occurred at low strengths (less tha 0.13 N) were all B type. These low strength failures did not result because of bonding conditions (force and temperature), but these failures were a result of the adhesion of the lead to the device itself. Thus, the integrity of the bonds made with this schedule is not primarily dependent on bonding conditions but on the quality of device purchased.

Bonding Large Format Devices

When devices larger than the Format 25 device or devices with asymmetric beam widths are bonded, the pressure at each beam varies as the bonding tool wobbles around the device.

Interface temperature is to be reviewed first. Temperature facilitates plastic flow of lead material and aids contaminant dispersion. Because lead material and contamination is not significantly different for large format devices than for Format 25 devices, the usable range of interface temperatures is the same.

A minimum pressure is necessary to form a bond; yet, that pressure is not to exceed a maximum above which deformation will be excessive. The minimum and maximum pressures were determined during the development of the bond envelope for Format 25 devices. The minimum force required is 450 g (4.4 N). The maximum force allowed is 950 g (9.31 N). The bond area for Format 25 devices is 8.77 square mils (0.0067 mm^2).

P min = 51.3 g/sq. mil (7.8 x $10^2 N/mn^2$);

P max = 108.3 g/sq. mil (1.6 x $10^3 N/mm^2$).

Exterior beam recieve more pressure that do interior beams. During bonding with a 1000 g tool load a device receives a minimum pressure of 32 g/sq. mil (12 N/mm^2) and a maximum of 73 g/sq. mil (28 N/mm^2) (Figure 25). Thus, to obtain the minimum required pressure, the tool load must be increased. The required force, F = 32/1000 X F = 51.3 or F = 1603 grams (15.7 N). Similarly

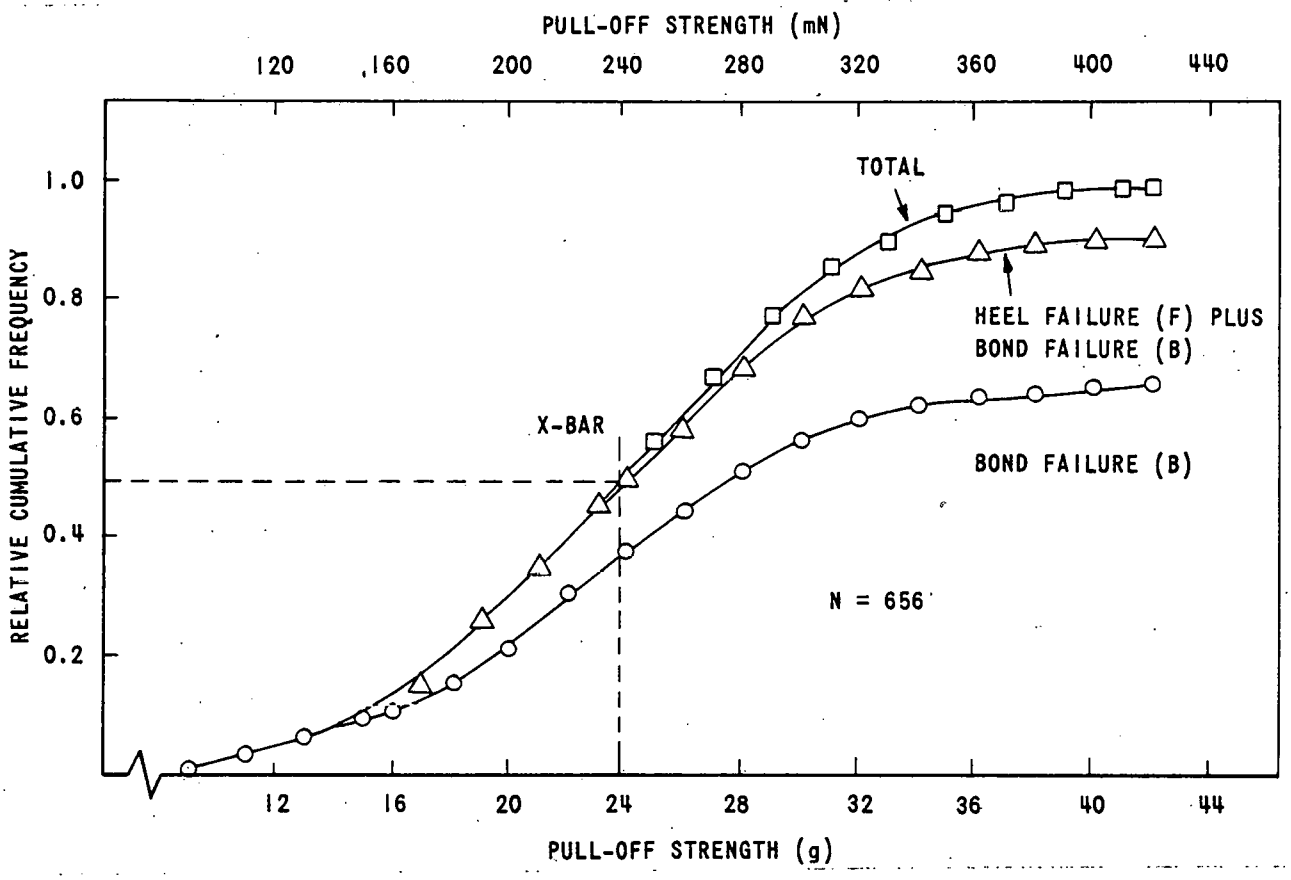

Figure 24. Distribution of Pull-off Strengths and Failure Modes for Format 25 Devices Bonded at Optimum Point

the maximum force (G) is 73/1000 X (G) = 108.3 or (G) = 1484 grams (14.6 N). For the case illustrated the maximum force allowed is less than the minimum required. The bond range G to F = -119 g (1.1 N)

To obtain a bond schedule for the Format 80 device, the maximum deformation and strength requirements must be relaxed. Because the minimum criteria of 51.3 grams/per square mil (19.5 N/mm^2) is required for bond completion, this criterion should not be changed. Format 25 devices can be extrapolated to larger format devices using Table 8.

Rework

Reworkability--the ability to remove defective BLDs and to replace them with good devices--is an important aspect of HMC technology. Five samples of Raytheon three-beam transistors were prepared to determine if removal of a defective transistor and subsequent re-bonding significantly affect the bond integrity of the reworked

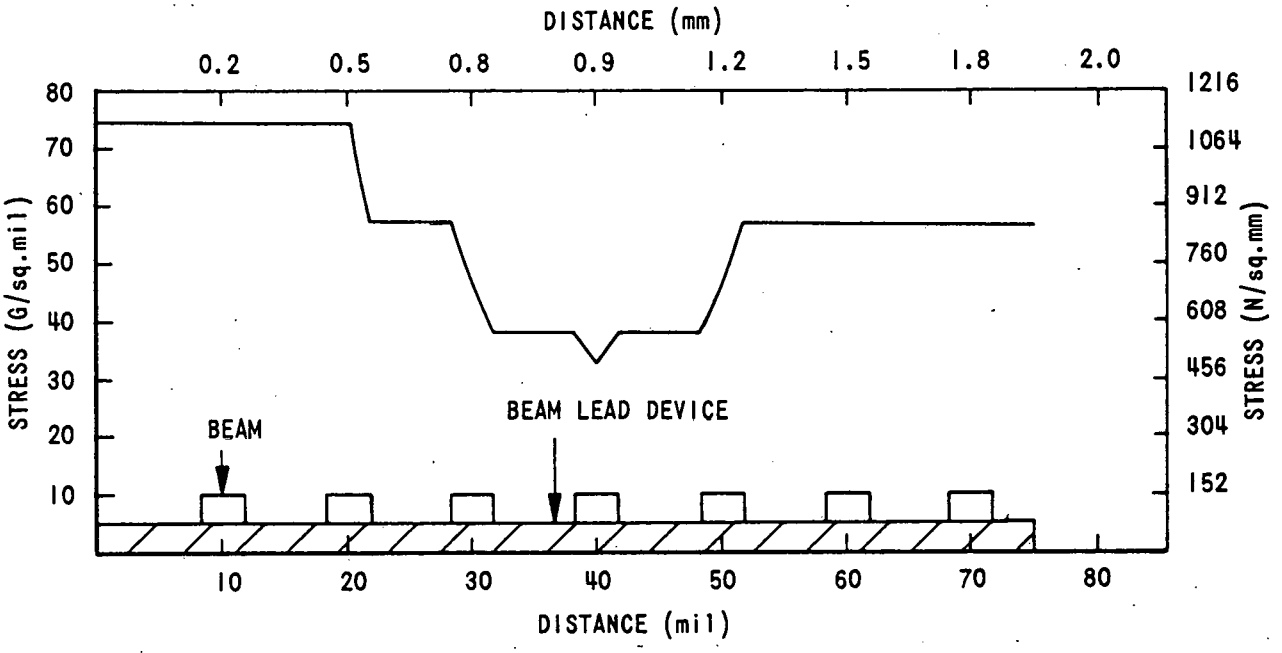

Figure 25. Format 80 Beam Stress During Bonding

device. The first sample, the control, consisted of nearly twenty transistors bonded on a substrate. The second sample was reworked once, the third reworked twice, the fourth reworked three times, and the fifth reworked three times, and the fifth reworked four times. The devices were removed with a Donovan rework tool which uses a blade to scrape the bonded beam leads from the substrate bonding pads. Each sample was tested using the pull-off technique and noting failure modes. All transistors used in preparing samples were from the same lot. The bonding parameters were constant for all samples.

The percentage of various failure modes is a function of rework (Figures 26,27, 28). A failure at the heel of a bond (Mode F) is nearly independent of rework. This indicate that the bonding parameters did not significantly change during bonding. Bond delaminations (D failures) began occurring at three reworks even though the average pull-off force was lowest at three reworks. At four reworks, more D failures occur. The average pull-off strength, was no greater than that applied at zero, one, and two reworks. The data, therefore, conclude that two stages of rework will not degrade bond strength. Verification of the results with three beam devices is shown in Figure 29. This shows that two reworks should be the limit for 14 beam devices.

One drawback exists with the scrape-off method of the BLD. The device is usually damaged so that failure analysis of the device

cannot be done. Additional work is needed to improve the method of removing the BLD.

Fine Wire Bonding

Applique components and the chromium-gold HMC conductor metallization can be intraconnected with gold wire, aluminum wire, or solder. Thermocompression bonded gold wire 0.007 inch (17.8 μm) and 0.001 inch (25 μm) diameter was selected to form the needed intraconnections on low frequency HMCs. HMCs made before the use of BLDs had ultrasonically bonded aluminum wire intraconnections to aluminum substrate metallization. Applying the ultrasonically bonded aluminum wires to a chromium-gold metallized HMC could result in degradation of the gold-aluminum bond. Gold-aluminum compounds are formed at the bond interface. Such degradation is dependent on the temperature and the quantity of gold. When the bond interface does not reach temperatures greater than 125°C and when the gold is less than 2.5 nm thick, satisfactory ultrasonic bonds of aluminum wire to gold conductors can be made. However, a gold wire TC bonded to a gold conductor has no limitations on the HMC operating temperature. Thermocompression gold wire bonding--commonly called ball bonding--is accomplished by feeding the gold wire through a bonding tool which has a capillary tip. A hydrogen torch is passed below the capillary tip. A ball is formed at the end of the wire approximately two to three times larger than the wire diameter. The ball is brought into contact with the gold conductor bonding pad on the HMC. Heat is applied to the bond interface through the bonding tool and the HMC substrate. Pressure is applied to the interface through the bonding tool. The combination of heat and pressure bonds the ball to the bonding pad. A second bond, the stitch bond, is made after lifting the tool and allowing the wire to feed through the capillary. The tool is then moved to the second bond location. The tool is brought into contact with the HMC or applique component metallization, and the stitch bond is formed as before by applying heat and pressure to the wire-metallization interface.

A wedge shape in the capillary tip sharply deforms the wire. After the second bond is made, the bonding tool is lifted. The wire then can be clamped so that the wire breaks at the maximum deformation in the bond without weakening the bond. A new ball is formed and ready.

Thermocompression wire bonding is similar to beam-lead bonding. Bonding parameters (such as cleanliness, bond time, deformation, and interface temperatures) and material parameters (such as wire and bond pad properties) determine the constraints in developing a bond schedule.

Table 8. Stress in BLDs With a 1000 g Tool Load

Format	Stress (A), Minimum g/mil^2 (N/mm^2)	Stress (B), Maximum g/mil^2 (N/mm^2)	Ratio of Stresses, A ÷ B
20	114 (1733)	114 (1733)	1
25	114 (1733)	114 (1733)	1
30	58 (882)	74 (1125)	1.28
35	58 (882)	73 (1110)	1.26
35T	40 (608)	128 (1946)	3.2
40	58 (882)	73 (1110)	1.26
45	58 (882)	73 (1110)	1.26
50	56 (851)	73 (1110)	1.3
55	56 (851)	73 (1110)	1.62
60	45 (684)	73 (1110)	1.62
65	39 (593)	79 (1201)	2.03
70	39 (593)	79 (1201)	2.03
80	32 (486)	73 (1110)	2.28
47	18 (274)	100 (1520)	5.56
54	58 (882)	114 (1733)	1.97
Ray.3	67 (1018)	134 (2037)	2.0
FUB	20 (304)	100 (1520)	5.0

Characterization of Parameters

Bond force, bond time, tool temperature, and substrate temperature were characterized for a Radiant Energy Systems Model 3000 TC wire bonder. Bond force calibrations are needed for both the ball and the stitch bonds. The force required to achieve a TC bond is different for the ball as compared to the stitch bond because the bond area is not the same for both bonds. Bond force was measured with a load cell (Figure 30), and the output of the load cell was plotted against the machine control settings (Figure 31). Bond time versus control settings is given in Table 9.

Tool and substrate temperatures were obtained using the apparatus shown in Figure 32. The results characterize substrate temperature (Figure 33) and tool temperature (Figure 34). The temperature

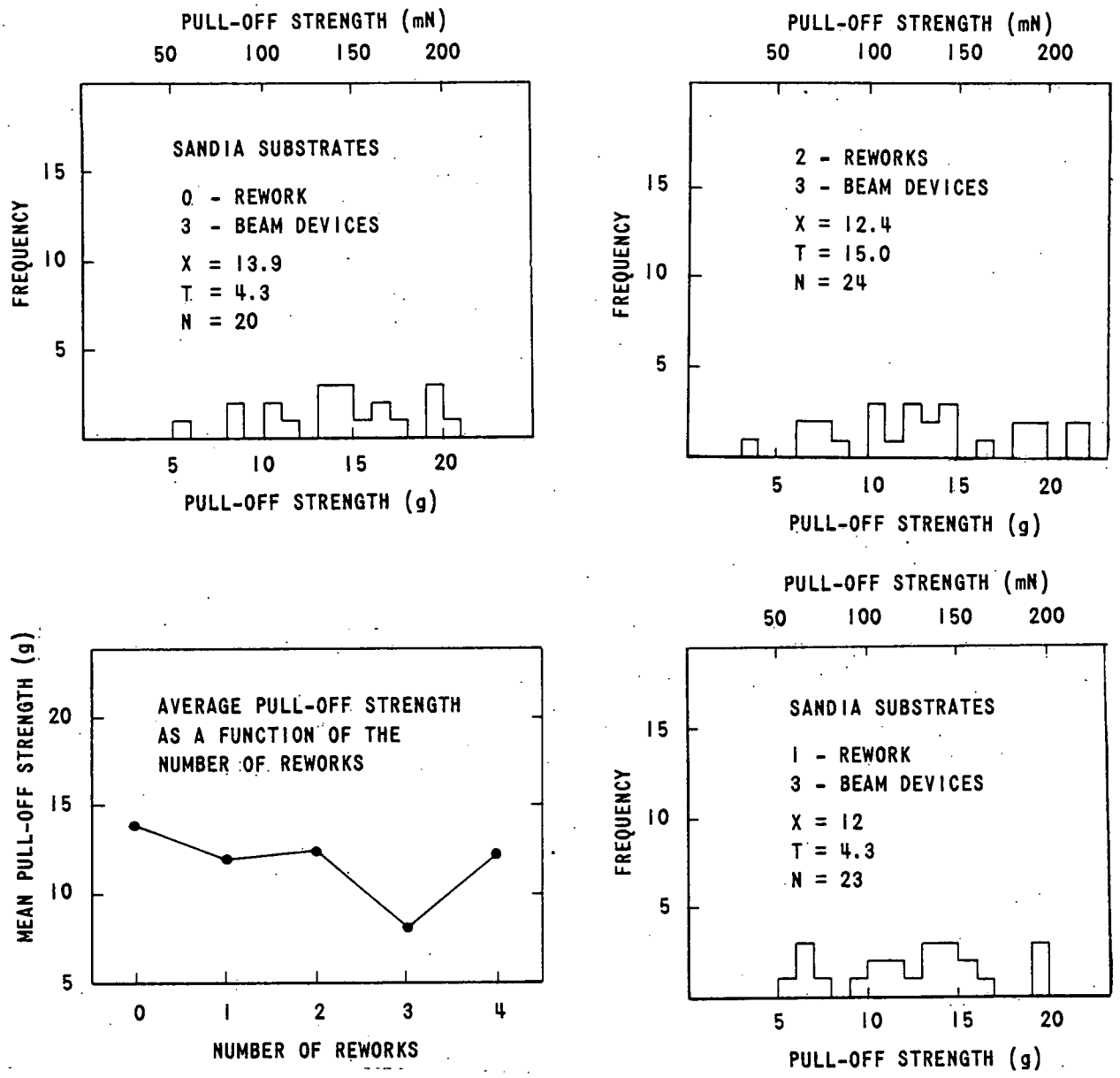

Figure 26. Rework of Three Beam Devices

measured on the metallization pad of a capacitor that had been epoxied to the substrate is nearly 15°C less that temperature measured on the bonding surface of the substrate.

The thin film thermocouple output for each tool temperature is recorded. A plot of interface temperature versus tool temperature is shown in Figure 35. Interface temperature increases slowly

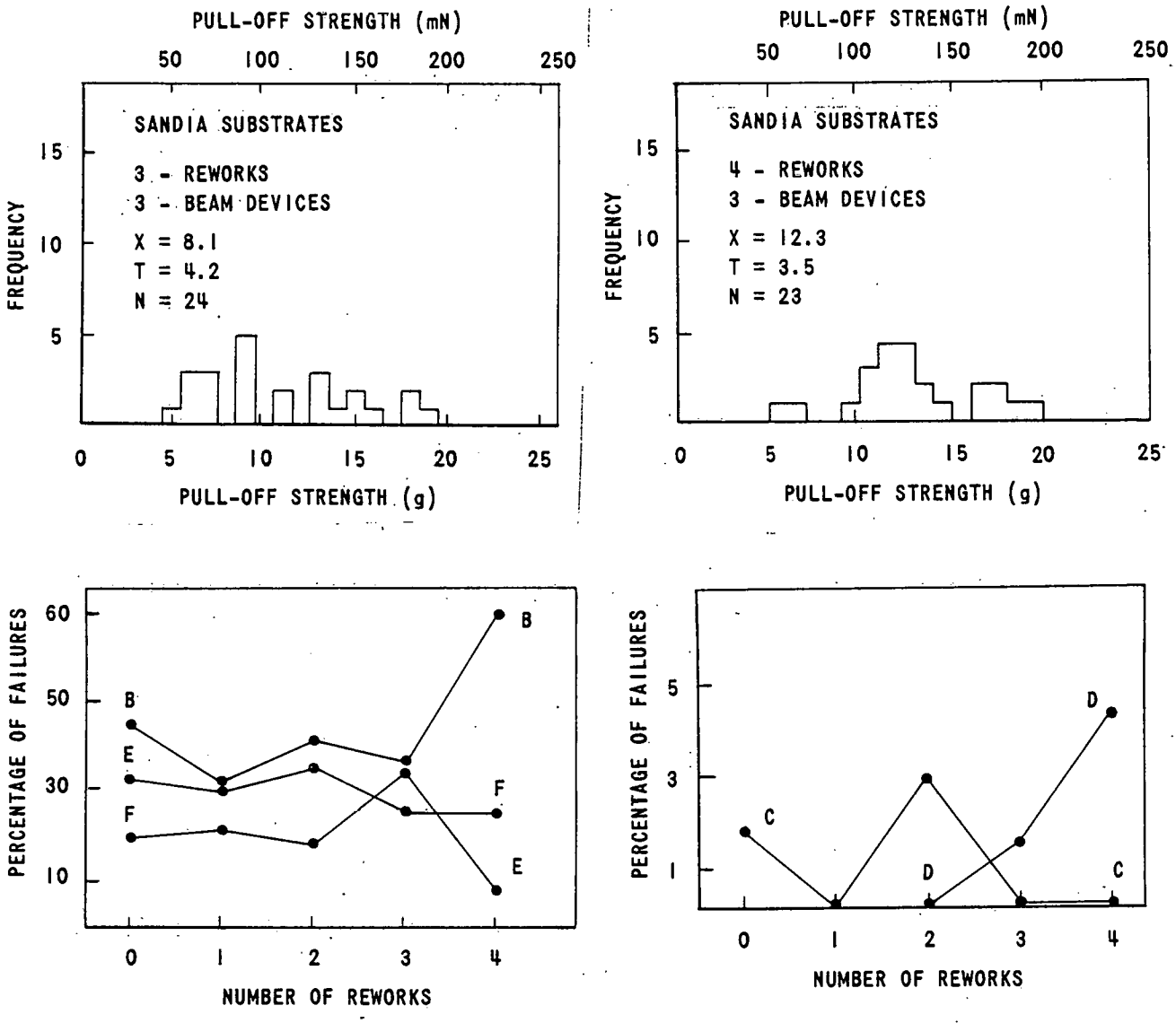

Figure 27. Rework of Three Beam Devices

after approximately 0.2 seconds from the time the gold ball is applied to the thin film thermocouple junction (Figure 35). Interface temperature can be plotted (Figure 36) by using the values of interface temperature, tool temperature, and substrate tempera- at 0.5 seconds (Figure 35) and determining the thermal characterization constant (A) from equation (2).

Text continued on page 72.

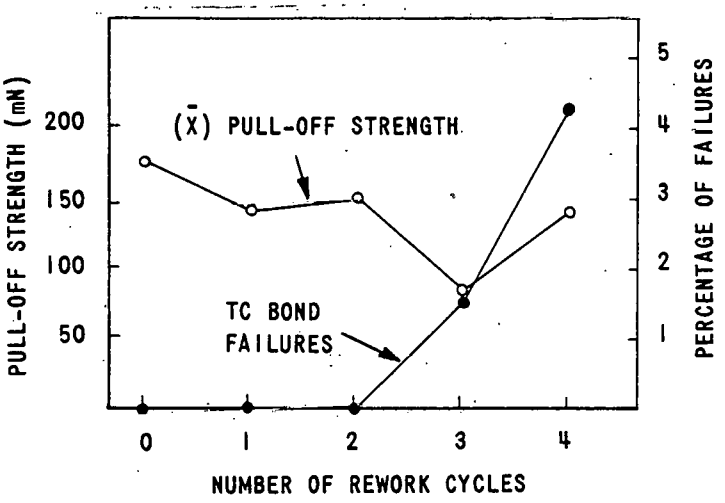

Figure 28. Rework of Three Beam Devices

Table 9. Bond Time Versus Control Settings for RES Model 3000 Bonder CE40854

First Bond				Second Bond			
Short		Long		Short		Long	
Set Point	Time (S)	Set Point	Time (S)	Set Point	Time (S)	Set Point	Time (S)
0	0.11	0	0.44	0	0	0	0.24
1	0.14	1	0.68	1	0	1	0.40
2	0.20	2	1.24	2	0.02	2	0.94
3	0.28	3	1.90	3	0.07	3	1.52
4	0.31	4	2.30	4	0.10	4	1.90
5	0.36	5	2.75	5	0.14	5	2.60
6	0.42	6	3.30	6	0.22	6	3.00
7	0.46	7	3.38	7	0.30	7	3.50
8	0.52	8	4.30	8	0.36	8	4.00
9	0.56	9	5.00	9	0.40	9	4.60
10	0.62	10	5.20	10	0.44	10	4.90

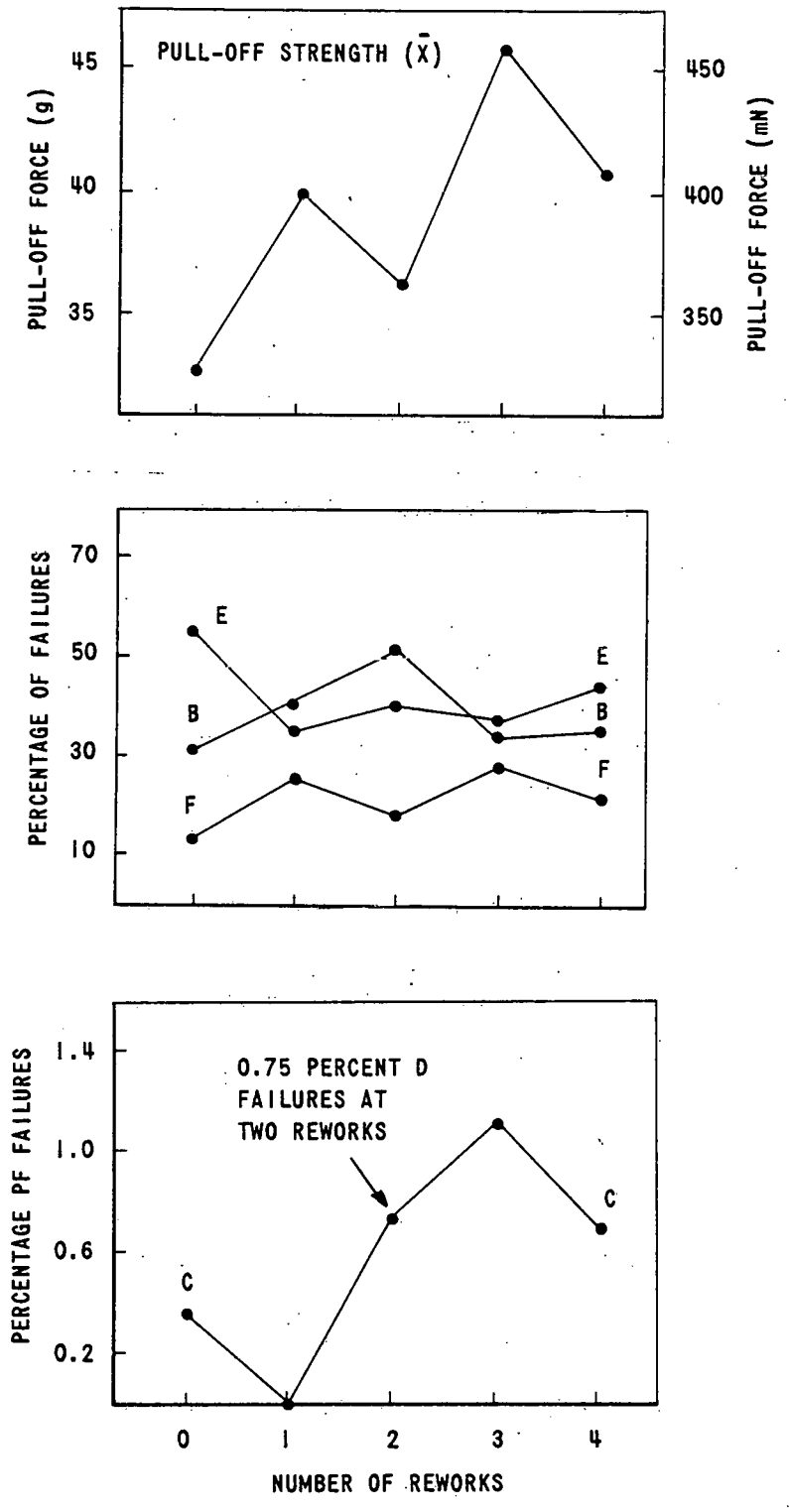

Figure 29. Rework of 14 Beam Devices

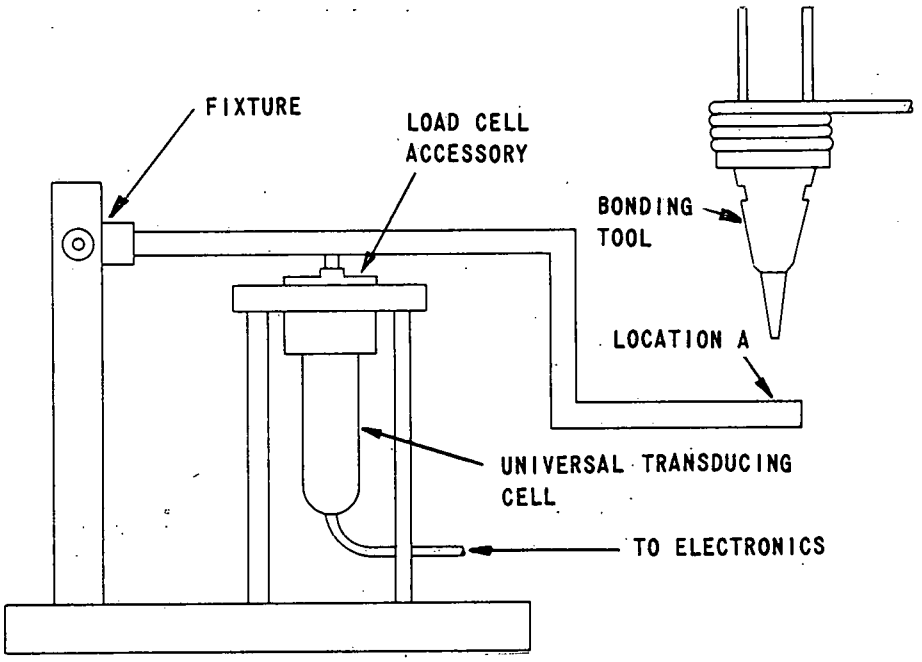

Figure 30. Bonding Force Measurement Apparatus

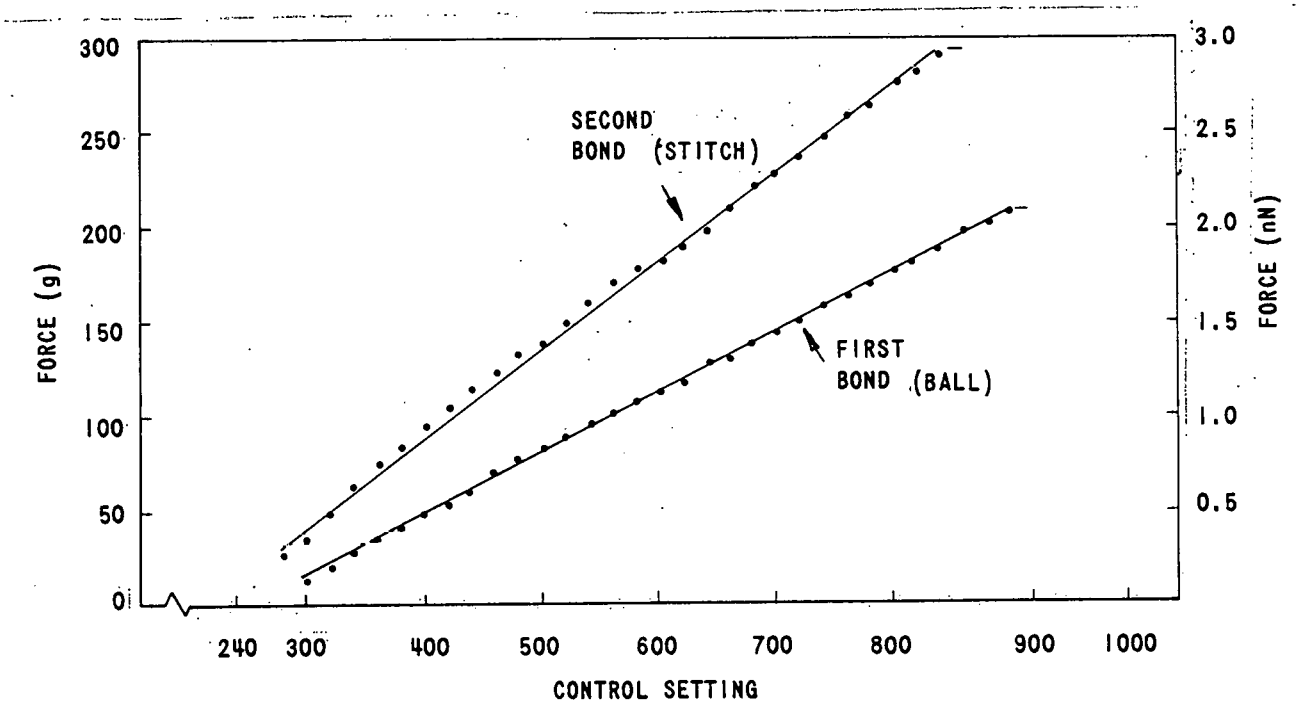

Figure 31. Bond Force Versus Bonder Setting

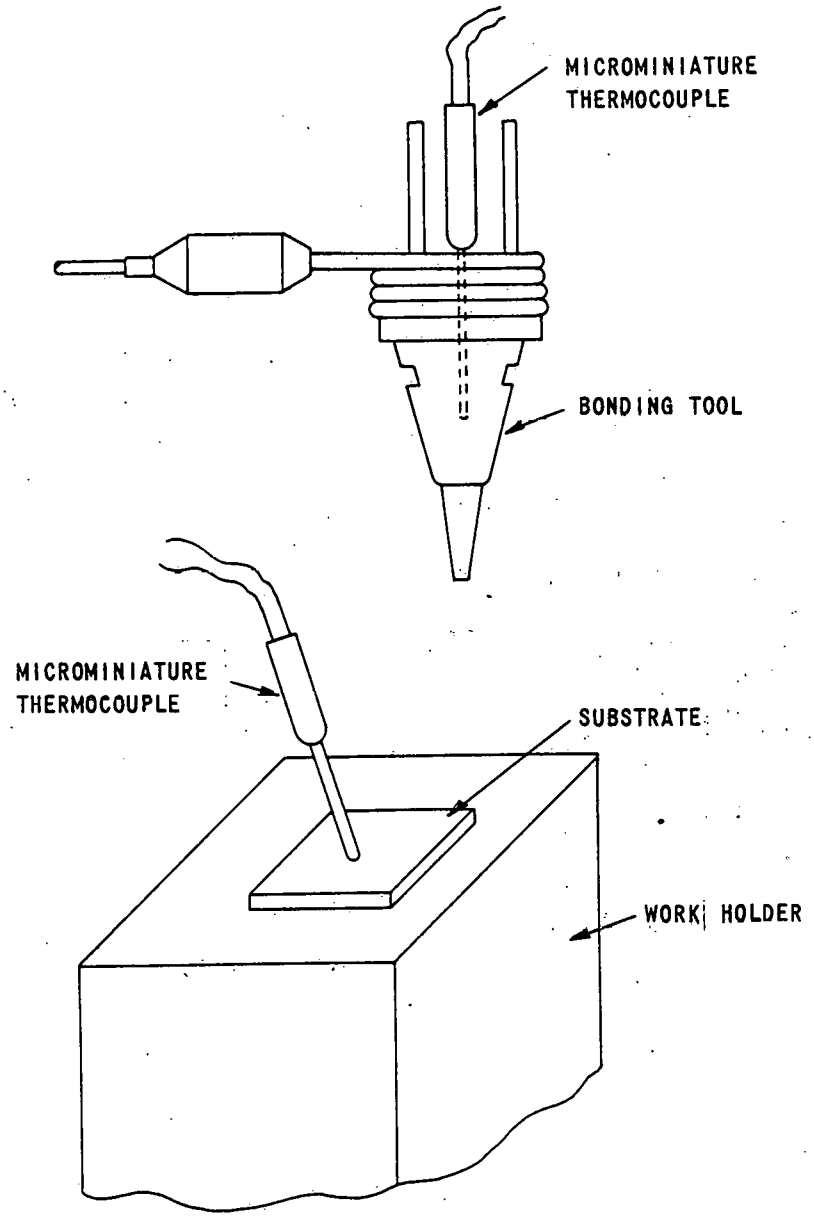

Figure 32. Wire Bonding Tool and Temperature Measurements

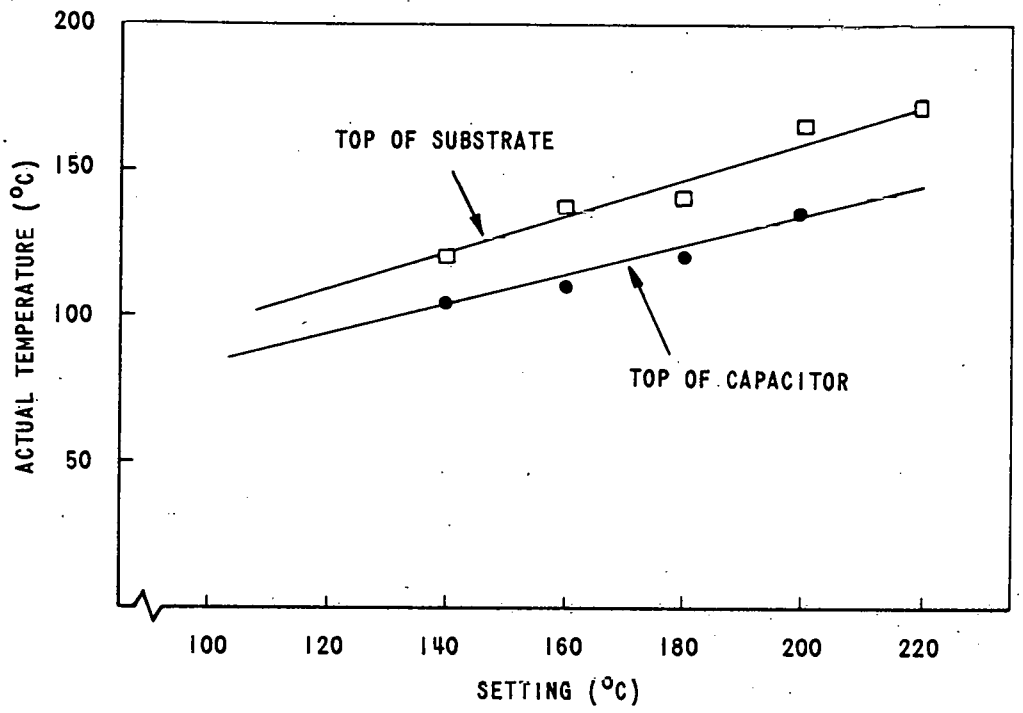

Figure 33. Wire Bonding Substrate Temperature Calibration

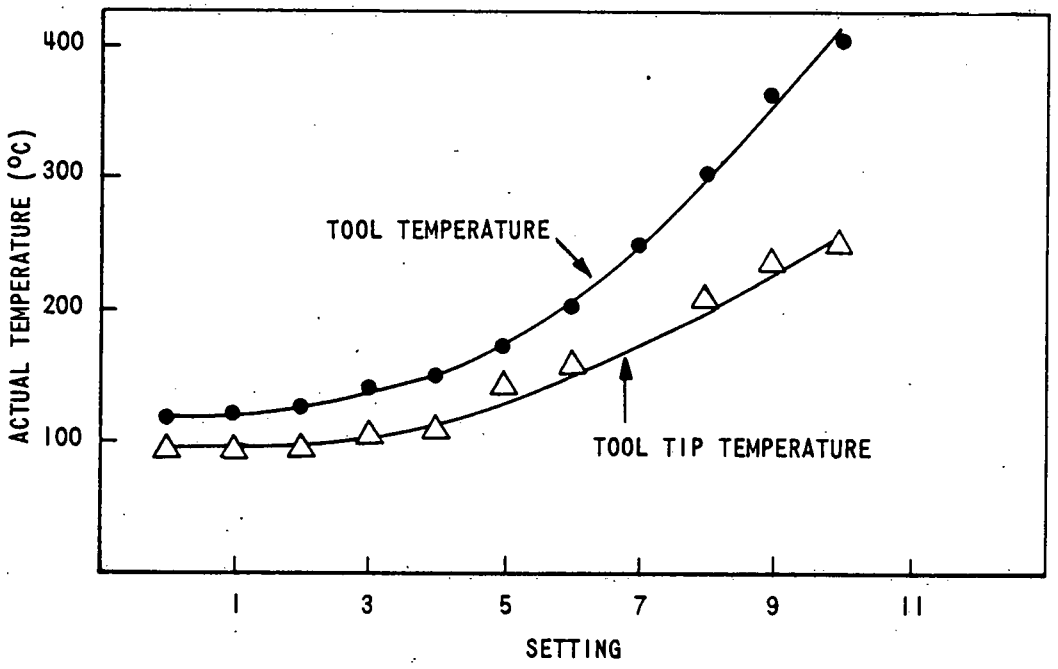

Figure 34. Wire Bonding Tool Temperature Calibration

Analysis of Bonding Parameters

Bond Time. Less than 0.1 second is needed to form gold-to-gold TC bond.[3] Therefore, the main concerns are that equilibrium be reached for interface temperature and that the equilibrium temperature be held for at least 0.1 second. The thermal characteristics of the bonding tool affect the time needed to reach thermal equilibrium. Metal tools reach equilibrium faster than glass or ceramic tools. Bond time must, therefore, be characterized for each tool type or configuration. When machine settings are calibrated to temperature (Table 9), bond time can be selected as the time to reach thermal equilibrium plus 0.1 seconds. A bond time of 0.3 seconds was selected for a titanium carbide tool that reached thermal equilibrium in 0.2 seconds (Figure 35).

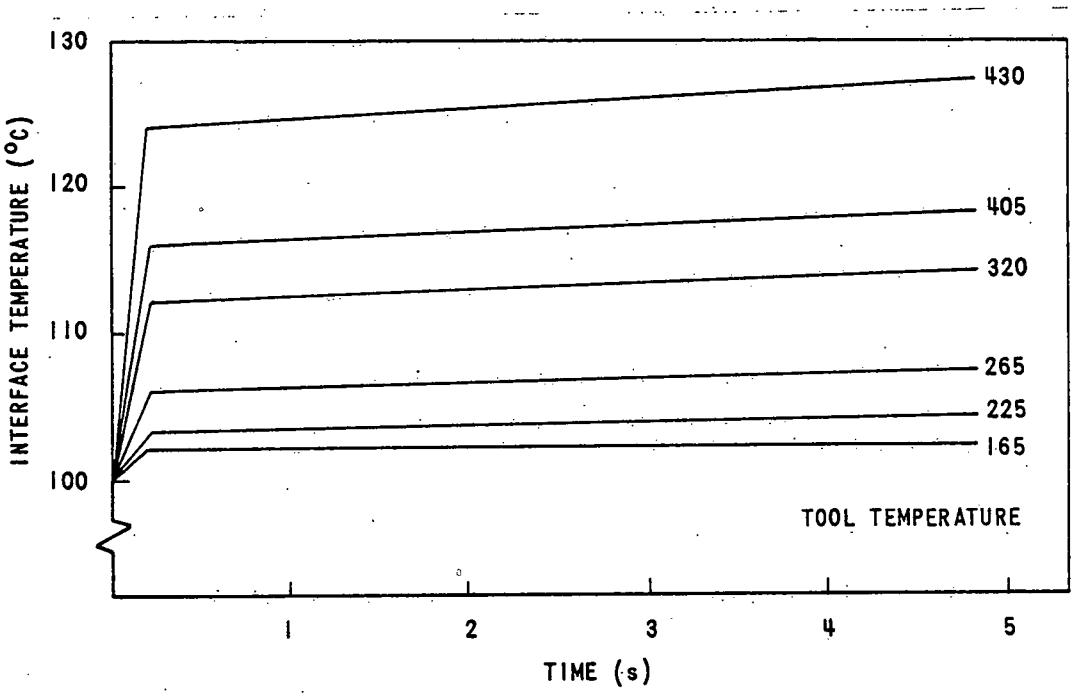

Figure 35. Wire Bonding Interface Temperature Versus Bond Time

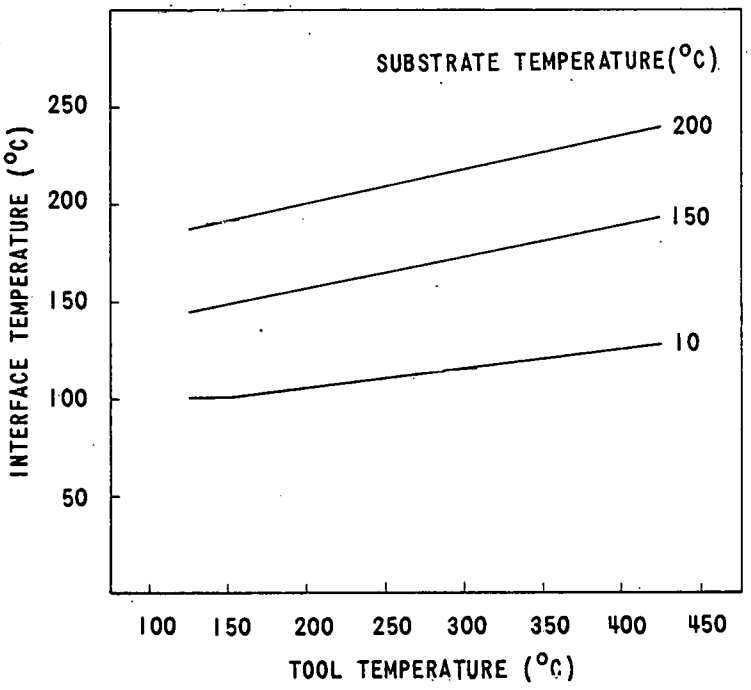

Figure 36. Wire Bonding Interface Versus Tool and Substrate Temperature

Bond Deformation. The act of deforming a bond disperses contaminants in the bond zone between the two materials that had been bonded. Deformation is controlled by the bond tool, bond configuration, and the amount of force applied to the bonding tool. The criteria for acceptable bond deformation is that all bonds must fail as wire breaks (Figure 37).

A wire failure indicates that the gold-to-gold TC bond is stronger than the wire that is being bonded. Wire strength depends on the amount of wire annealing. This includes processing from bulk to wire form. Gold wire can be bought in various elongations (degrees of annealing). Figure 38 shows how wire tensile strength varies with elongation before bonding.

One percent nominal elongation 0.003 inch (76 μm) wire has 16 grams tensile strength; 6 percent elongation wire has 7 grams tensile strength. The tensile strength of 1 to 8 percent elongation wire was reduced to nearly 5 grams tensile strength after bonding (Figure 38).

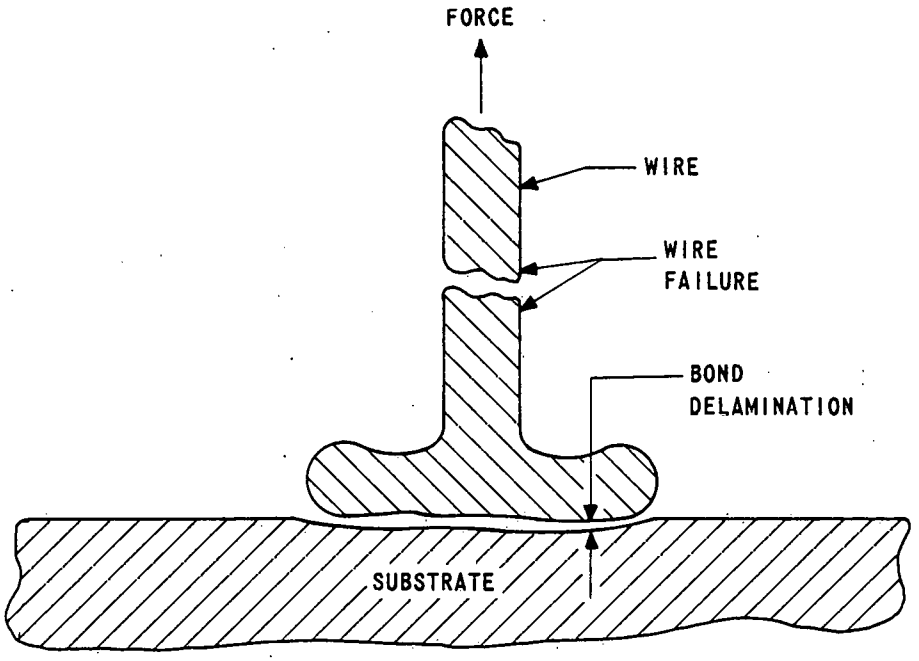

Figure 37. Wire Bond Criteria

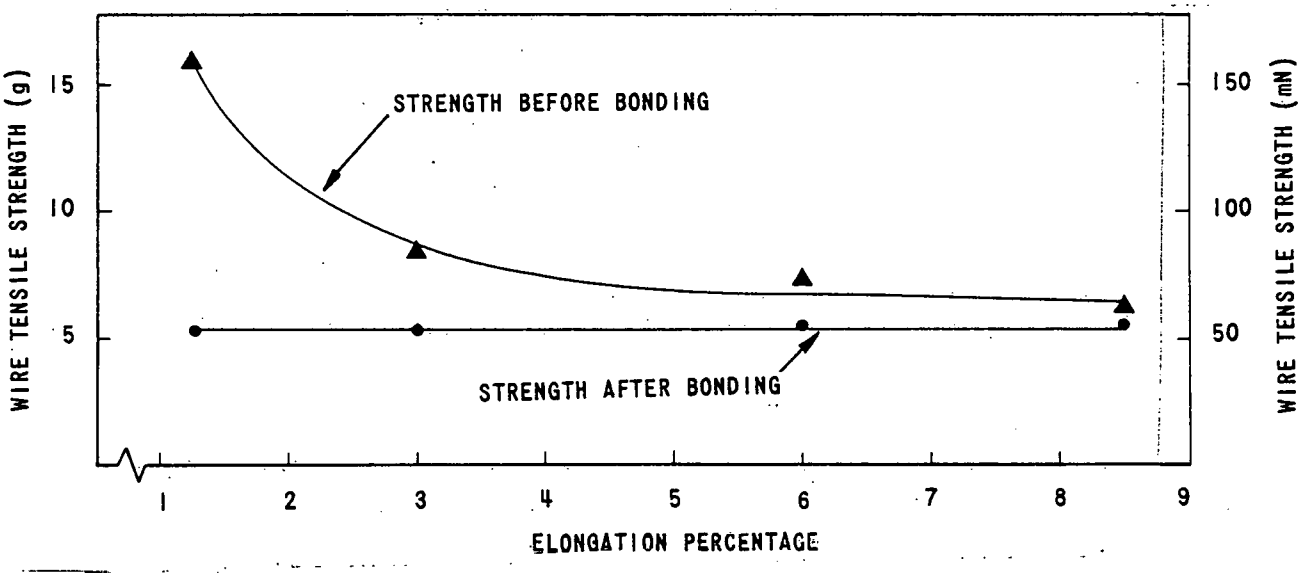

Figure 38. Independence of Wire Strength on Elongation

An investigation of gold wire annealing properties showed that wire subjected to temperature above 100°C decreases to 40 percent in tensile strength (Figure 39). Above 250°C the wire is essentially in the dead soft state. No further decreases in tensile strength occur. The temperature developed in the gold wire from flame off was determined as a function of distance from the ball (Figure 40). At distances up to 0.1 inch (2.5 mm) from the ball, the wire reaches more than 100°C. The bonding tool is heated during bonding to at least 100°C, and some annealing takes place after the flame-off operation is complete. Because the bonding operation causes gold wire to reach a dead soft state, wire elongation was eliminated as a process variable.

Bond configuration influences bond integrity. Varying the bond area can cause inconsistent bonding when bond force is held constant. The consistency of ball deformation with the RES Model 3000 bonder was evaluated in the following procedure. Three bond samples were produced from 0.001 inch (25 µm) wire. The first (large ball case) consisted of 56 bonds. All bonds were produced so that deformed ball size should exceed 0.005 inch (0.127 mm). The second sample (small ball case) consisted of 102 bonds. These bonds were produced to have a deformed ball size less than 0.005 inch (0.127 mm). The third sample, 20 bonds, were produced five days after the second sample.

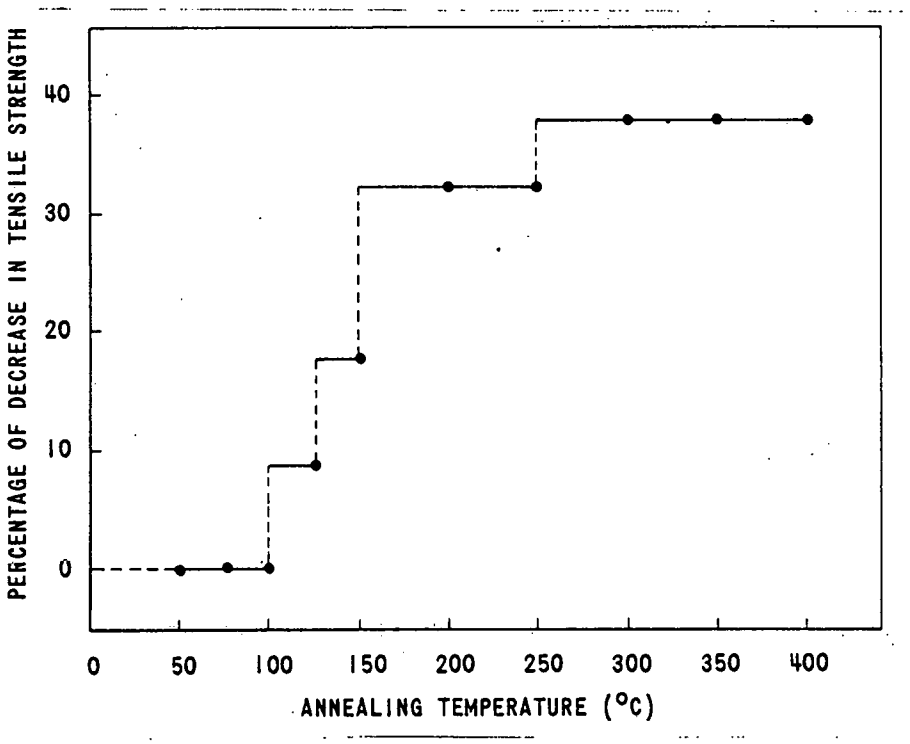

Figure 39. Annealing Properties of 3-Mil 99.99 Percent Gold Wire

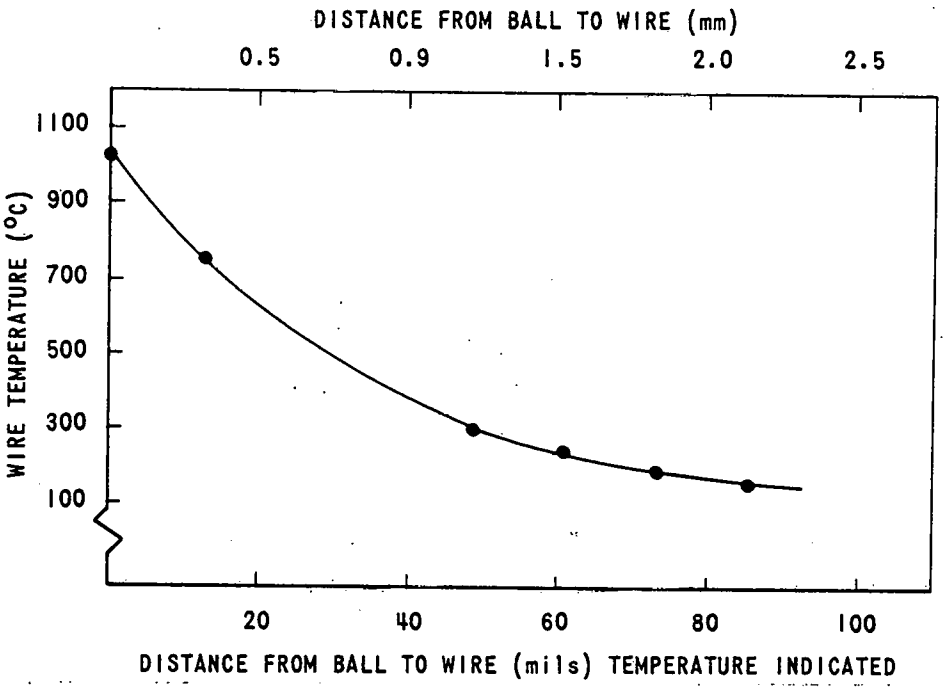

Figure 40. Annealing During Bonding

During this five day period the machine was not operated and no adjustments were made before bonding the sample. The deformed ball size distributions are shown in Figure 41 and Table 10.

Table 10. Deformed Ball Size Distributions

Sample	Mean Inches (mm)	Sigma Inches (mm)	Size
1 (large)	0.0057 (14)	0.00045 (110)	56
2 (small)	0.0038 (96)	0.00022 (6)	102
3 (small)	0.0040 (100)	0.00024 (6)	20

The tests indicate that as ball size is decreased, the variance of the sample decreases.

Over the five day period between the two samples, some flame-off parameter must have changed. The shift indicates that consistency will require occasional adjustments of flame-off parameters. The ball diameter should be less than the bonding tool tip diameter. This ensures proper ball size before bonding. After flame-off the ball should be hidden by the bonding tool.

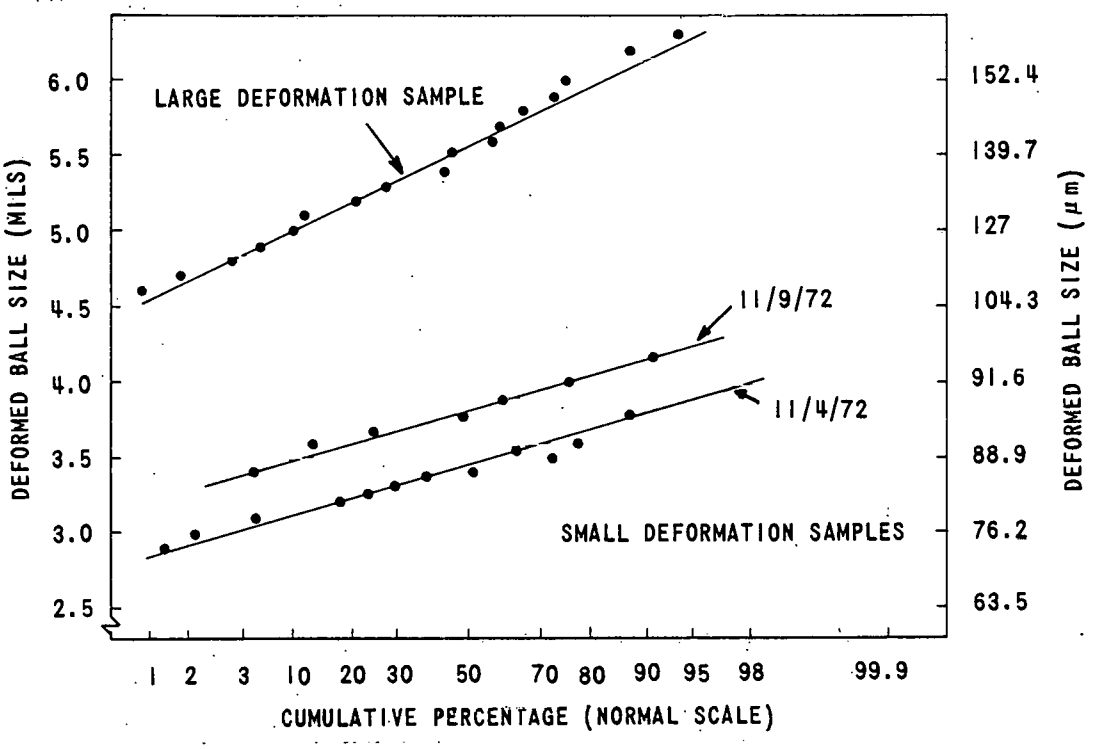

Figure 41. Ball Deformation Distributions

Samples 1 (large ball) and 2 (small ball) were pulled to destruction. Failure mode and fracture strength were recorded (Figure 42).

The small ball distribution (sample 2) is clearly normal. The distribution is a straight line on normal probability paper. The large ball distribution (sample 1) is not linear and therefore, not normal. A closer look at failure modes associated with the large ball sample indicated wire and neck failures. A wire failure is a fracture which occurs anywhere in the wire away from the bond deformation. A neck failure is a failure which occurs at the deformed area just above the ball. The bimodal characteristics of the large ball sample indicate that large ball size can result from two conditions. First, during flame-off a large ball can be produced. Second, a small ball produced during flame-off can be excessively deformed during bonding. The first condition should produce bonds which fail only in the wire. Bonds produced by the second condition would likely fail as neck failures. The two distributions and the the distribution for small ball bonds are shown in Figure 43 and tabulated in Table 11. All bonds of the small ball sample failed as wire failures.

Table 11. Strength Distributions

Sample	Mean (mN)	Sigma (mN)	Sample Size
1-Wire	54	4.4	18
1-Neck	47	10.5	38
2 (Small)	57	0.24	102

Sample 1-W (Large ball, wire failures) and Sample 2 (small ball) are normal (Figure 43). The small ball distribution is approximately 0.5 grams stronger than the large ball case. The large ball-neck failure case (1-N) is a skewed distribution. The probability of bonds with low strength is higher than that predicted by a normal distribution. Table 12 summarizes bond integrity as a function of stress.

Table 12. Bond Integrity

Sample	Failure Mode	Stress Level*		
		5 gram (50 mN)	4 gram (40 mN)	1 gram (10 mN)
Small ball	Wire	0.01	0**	0**
Large ball	Wire	17.00	0**	0**
Large ball	Neck	47.00	22	1.2

*This percentage is expected to fail at the the given stress level or at a lower stress.
**The minimum strength of fully annealed 99.99 percent gold, 1 mil (25 μm) diameter wire is 4.0 grams (39 mN) as reported by Secon Metals Corporation.

Neck failures should not be allowed. Strengths ranging from 2.1 to 6.1 g (20 to 60 mN) would allow 1.2 percent of the sample to fail at strengths of less than a gram. The small ball and large ball-wire failures are acceptable. In both cases the minimum strength predicted is a 4 grams. The problem in the large ball case is determining nondestructively that the ball has not been

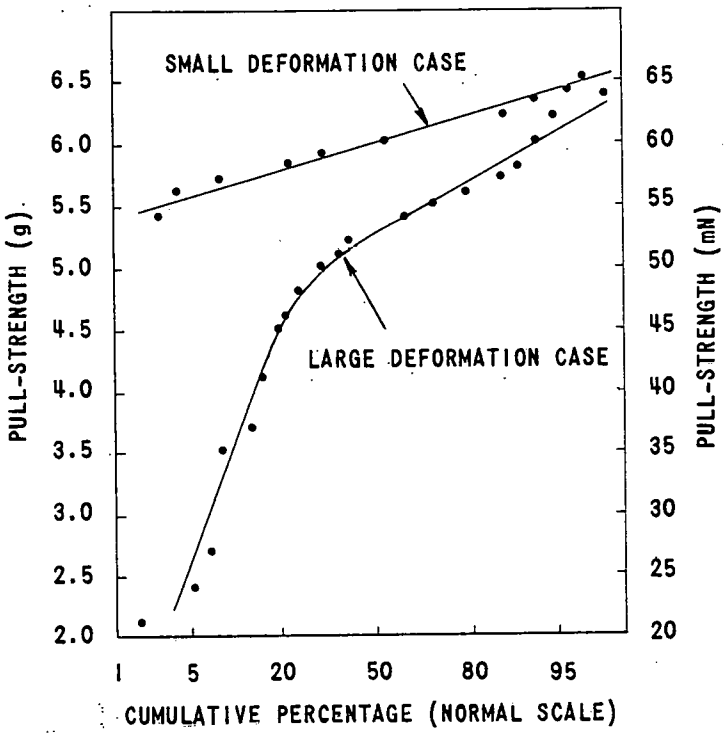

Figure 42. Pull-strength Distribution Versus Ball Deformation

overly deformed. A visual criteria based on the ratio of ball diameter to ball thickness would be adequate. Another possible test would be a nondestructive pull to a stress level of at least 1 gram (10 mN) In either case, the bonder should be set to produce balls less than five wire diameters in size after flame off.

Flame-off, tip orifice size, wire size and tension, the cutting speed, the thermal characteristics of the flame, distance from flame to wire, and the bonding tool affect ball size. Figure 44 shows the results of improper set-up of bonder flame-off. The capillary must remain clean in order for the wire to pass through freely. This keeps constant tension on the wire. In one study, bonding in a normal factory environment resulted in capillary plugging about every 30 meters of wire. Capillaries in clean conditions remained free and ran for 15 km.[17]

The same study showed that capillary plugging occurs about 1.2 m before wire breakage and the resulting change in wire tension causes changes in ball size. Therefore, according to the recent study, work increases the probability of a defective bond.

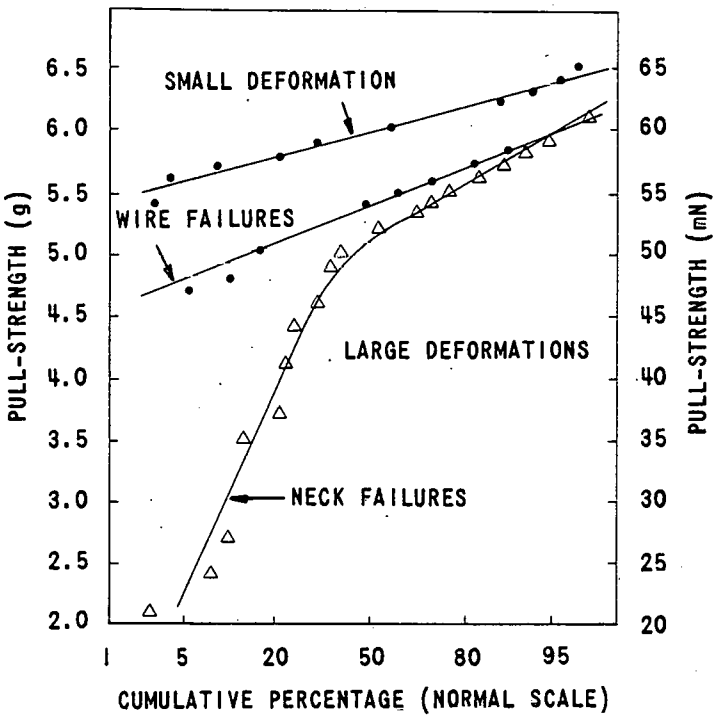

Figure 43. Pull-strength Distributions by Failure Mode

Capillary material affects wire tension by influencing the friction between the wire and the capillary. Figure 45 shows scanning electron-microscopic views of glass, ceramic (Al_2O_3), and tungsten-carbide capillaries. It might be expected that the smoother glass capillaries would result in less plugging than the rougher titanium carbide or ceramic capillaries. However, glass capillaries can plug after 5,000 bonds. Ceramic capillaries might not plug up to 25,000 bonds.[17] Evidentally the smooth glass walls increase the friction because of a larger contact surface to the wire as compared to the rougher ceramic or tungsten-carbide tools.

Bonding Surface Cleanliness

The cleanliness of the surfaces being bonded affects bond reliability. During HMC processing the tantalum nitride-chromium-gold coated ceramic substrates are exposed to 300°C for 2 hours. This stablizes the tantalum nitride resistors. HMCs are also handled before TC bonding. Studies were made to evaluate the effects of resistor stabilization, time-temperature, and substrate cleanliness as functions of TC bondability.

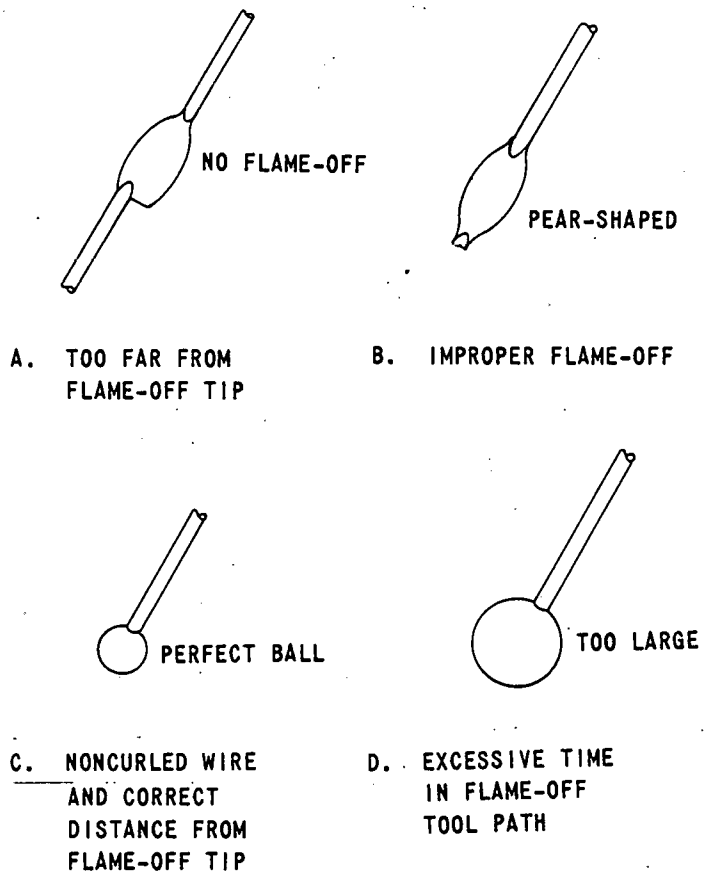

Figure 44. Bonder Setup Effects on Ball Size

The bondability of tantalum-nitride-chromium-gold coated substrates was measured with respect to tantalum nitride stabilization temperatures. The bondability was determined as the percent of bond delamination failures between ball bonds and the substrate gold surface (Figure 46). The substrate gold thickness was nominally 1 nm. Increasing the gold thickness to 3 nm improved film bondability to an acceptable zero percent occurrence of delamination. A potassium-iodine and iodine etch followed the resistor stabilization.

Further evaluation related the range of bonding force (grams) and interface temperature (°C) to stabilization process variables. Substrates with tantalum-nitride resistors and chromium-gold conductors were exposed to 250 to 400°C for varying times.

Resistor values were measured after stabilization and after 750 hours at 125°C; The stability was calculated in percentage of the change in resistor value the test. The results of that study

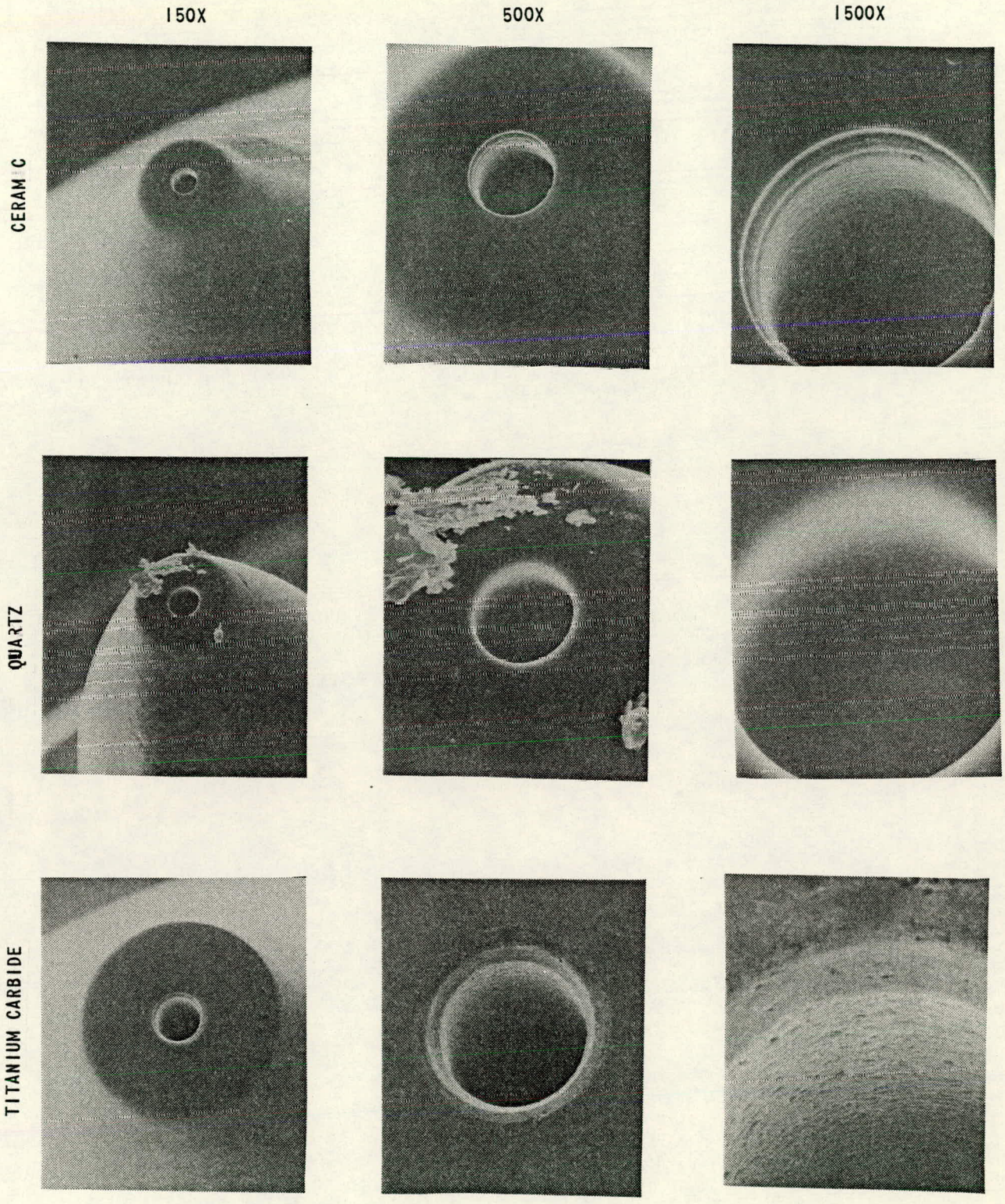

Figure 45. SEM Views of Capillaries

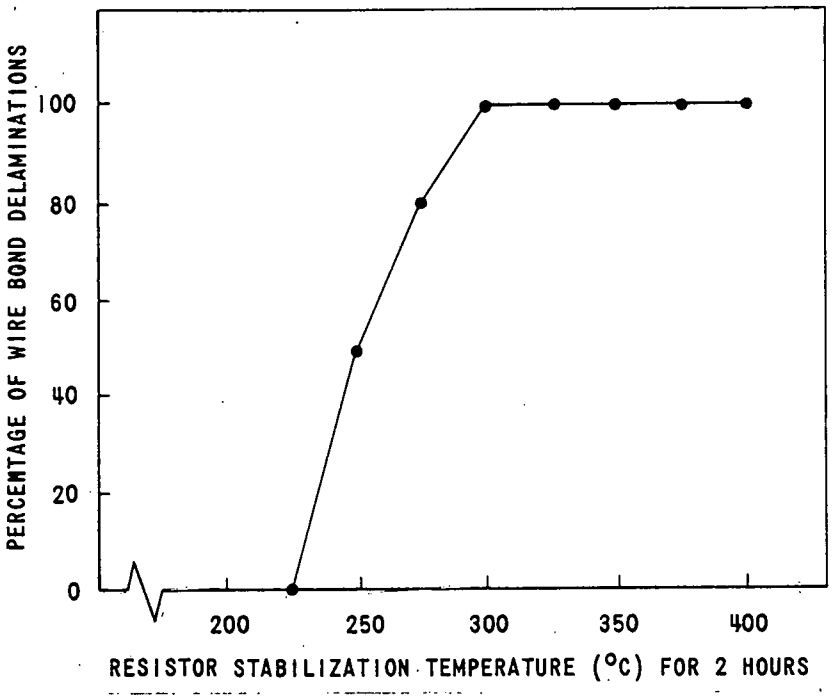

Figure 46. Wire Bond Delamination Versus Resistor Stabilization Temperature

are shown in Table 13. The 300°C, 2 hour stabilization gives adequate bondability and resistor stability. Later work has shown that the source of bond degradation was the chromium oxide which had formed on the gold surface during resistor stabilization. Ceric ammonium nitrate was effective in removing the chromium oxide and restoring bondability.[11,18]

Five different test samples were studied to evaluate the effects of substrate cleaning on wire TC bonding.

- Uncleaned substrates had been stored for 2 weeks in a plastic container after gold deposition.
- Substrates were cleaned by an organic removal process (SS289354, Method 1).[19]
- Substrates were cleaned by Method 1 with an addition of a dilute HCl wash before drying (Method 2).
- Substrates were sawed and cleaned per SS289365.[19]
- Substrates purposely were contaminated with fingerprints.

Table 13. Film Properties Versus Stabilization

Stabilization*		Resistor Stability	Bondability
Temperature °C	Time (Hours)	Stability** (Percentage)	Grams °C***
250	2	0.68	6475
300	2	0.06	6325
350	2	0.03	1350
400	1	0.03	1350

*Data taken after 750 hours at 125°C.
**Stability is required to be less than 0.2 percent over 1000 hours of testing.
***Area of bonding envelope.

Note: After stabilization at 400°C for 0.5 hours, gold film sheet resistance increases by 60 percent and film hardness increases by 2.7 percent.

The bonder settings used were not necessarily the optimum for the wire diameter not the substrates. The substrates used were obtained from in-house and from an outside vendor. The results indicate that substrates adequately protected from fingerprints require no cleaning (Tables 14 and 15). Method 1 is effective in restoring bondability to handled substrates.

Bond Schedule Development

A bonding envelope was defined for the following combinations of metallization: gold bonding pads on HMCs, chip capacitor terminations, and chip-on-tab device metallization. Constraints placed on the bond envelope result from machine limitations, TC bond failures during testing, and the softening point of the Ablefilm 517 epoxy. The epoxy was used to glue applique ceramic capacitors to the HMC substrates. Figure 47 shows the different bond envelopes for intraconnecting a chip capacitors to gold metallization on the HMC substrate.

The ball bond is machine limited to 200 grams (1.96 N) bonding force. The stitch was limited to 300 grams (2.9 N). Bond delaminations of capacitor metallization ball bonds occur for

Table 14. Evaluation of Cleaning Vendor Substrates

Cleaning Method*	Wire Diameter (Inch) (μm)	Mean (Grams) (mN)	Sigma (Grams) (mN)	Sample Size	Bond Pulled	Number of Wire Failures
Uncleaned**	0.001 (25.4)	5.6 (53.92)	0.38 (3.73)	44	Ball	25
Method 1	0.001 (25.4)	5.2 (51.00)	0.38 (3.73)	22	Ball	22
Method 2	0.001 (25.4)	5.0 (49.04)	0.77 (7.55)	21	Ball	21
Sawed and Cleaned	0.001 (54.2)	5.9 (57.86)	0.55 (5.39)	50	Ball	50
Handled		No Bonds Achieved				
Handled and Cleaned	0.001 (35.4)	5.7 (55.90)	0.78 (7.65)	44	Ball	40
Uncleaned	0.001 (25.4)	5.7 (55.90)	0.43 (4.22)	54	Stitch	54
Method 1	0.001 (25.4)	5.5 (53.94)	0.55 (5.39)	18	Stitch	18
Method 2	0.001 (25.4)	5.0 (49.04)	0.38 (3.73)	17	Stitch	19
Sawed and Cleaned	0.001 (25.4)	6.3 (61.78)	0.50 (4.90)	45	Stitch	45
Handled		No Bonds Achieved				
Handled and Cleaned	0.001 (25.4)	6.3 (61.78)	0.41 4.02)	50	Stitch	50
Uncleaned	0.003 (76.2)	50.5 (495.25)	3.0 (29.42)	33	Ball	33
Method 1	0.003 (76.2)	49.8 (488.39)	1.8 (17.65)	29	Ball	29
Method 2	0.003 (76.2)	51.0 (500.16)	1.9 (18.63)	29	Ball	29
Uncleaned	0.003 (76.2)	53.2 (521.73)	3.0 (29.42)	32	Stitch	32
Method 1	0.003 (76.2)	51.3 (503.10)	2.6 (25.50)	27	Stitch	27
Method 2	0.003 (76.2)	52.5 (514.87)	1.5 (14.71)	32	Stitch	32

*In all cases there were no lift or peel bond failures
**Had nineteen neck failures

Table 15. Evaluation of In-House Substrates

Cleaning* Method	Mean Grams (mN)	Sigma Grams (mN)	Sample Size	Bond Pulled	Neck Failures	Number of Wire Failures
1. Uncleaned	5.2 (51.00)	0.38 (3.73)	25	Ball	0	25
2. Method 1	6.2 (60.80)	0.49 (4.80)	44	Ball	0	44
3. Method 2**	5.3 (51.98)	0.29 (2.84)	46	Ball	4	30
4. Uncleaned	5.3 (51.98)	0.36 (3.53)	22	Stitch	0	22
5. Method 1	5.7 (56.89)	0.86 (8.43)	40	Stitch	0	40
6. Method 2	5.1 (50.02)	0.27 (2.45)	25	Stitch	2	23
7. Uncleaned	48.1 (471.72)	2.8 (27.46)	26	Ball	0	26
8. Method 1	49.7 (487.41)	3.0 (29.42)	34	Ball	1	33
9. Method 2	49.4 (484.47)	1.8 (17.65)	14	Ball	2	12
10. Uncleaned***	48.6 (477.62)	5.4 (52.96)	23	Stitch	0	22
11. Method 1	50.5 (495.25)	3.6 (35.30)	18	Stitch	2	16
12. Method 2 (483.50)	49.2 (43.15)	4.4	12	Stitch	4	8

*Test 1-6 used wire with 0.001 inch (25.4 μm) diameter; tests used wire with 0.003 (76.2 μm) diameter.
**Had two lift failures.
***Had one lift failure.

parameter values below a line connecting 140 grams (1.37 N), 110°C to 85 grams (0.83 N), 170°C. Bond schedule development results in the following bonding envelopes (Figure 48, 49): Sandia-Bendix gold HMC metallization, vendor gold HMC metallization, chip-on-tab metallization, and capacitor terminations. All combinations of metallization which can be TC bonded in Energy Research Development Administration (ERDA) HMCs are given in Figure 50. Histograms for the optimized bond parameters are given in Figure 51.

Text continued on page 90.

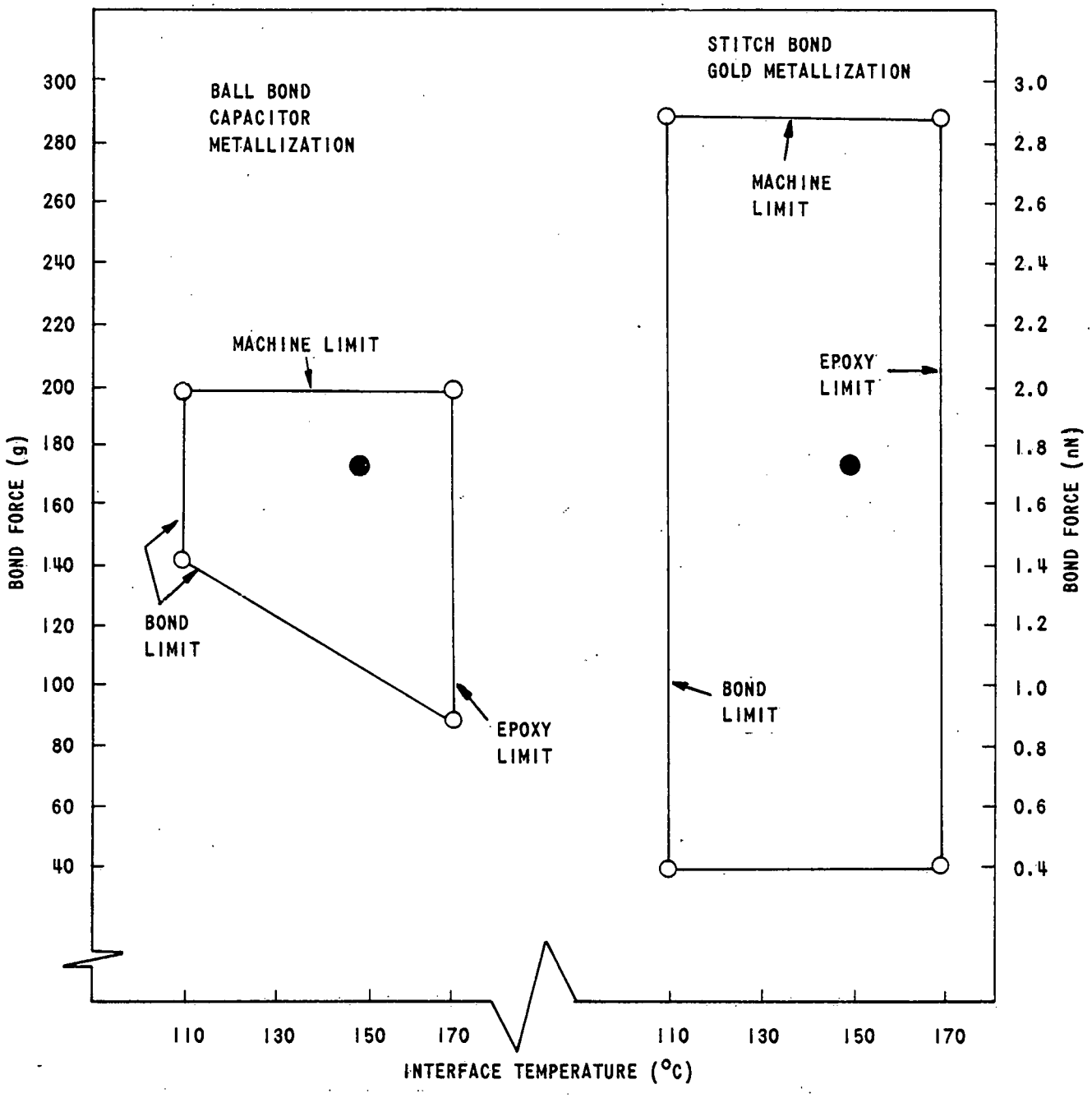

Figure 47. Capacitor Versus Evaporated Gold Metallizations Within the Wire Bond Envelope

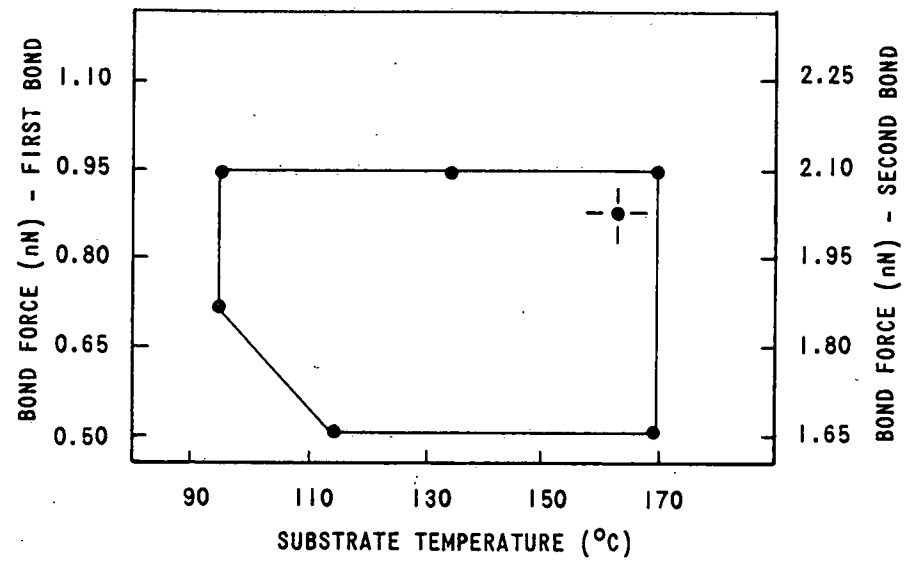

A. VENDOR

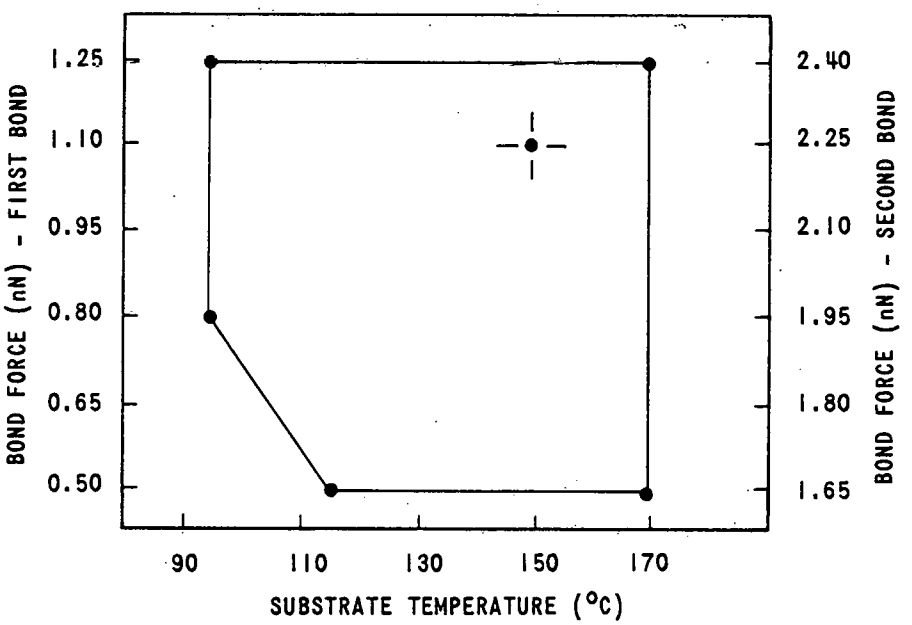

B. SANDIA-BENDIX (ERDA)

Figure 48. Vendor and ERDA HMC Metallizations Within an Optimized Bond Envelope

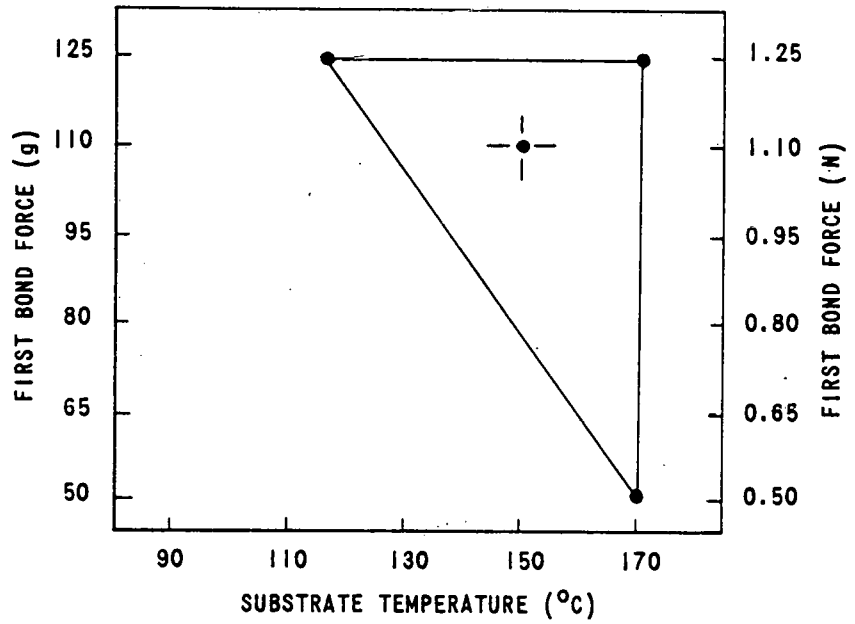

A. ACTIVE DEVICE METALLIZATION

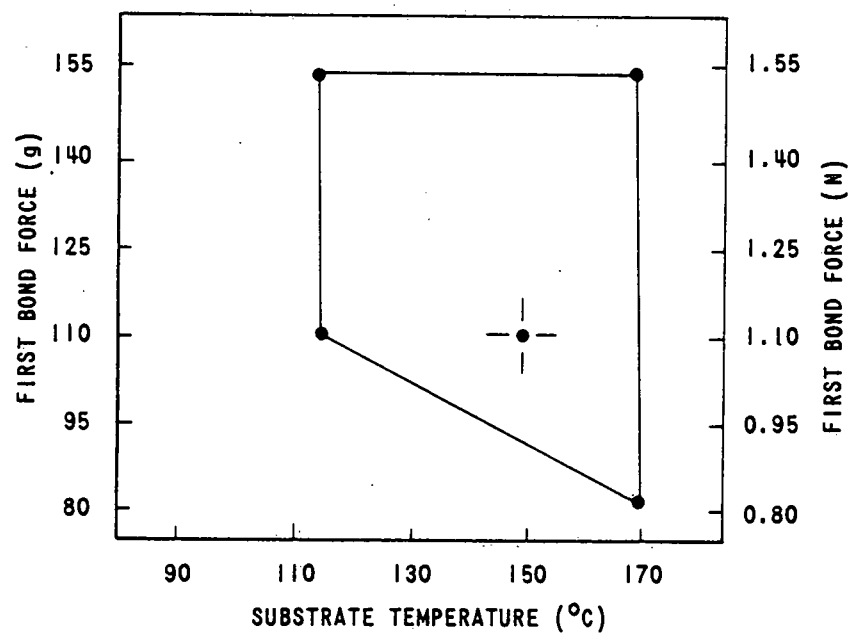

B. CAPACITOR METALLIZATION

Figure 49. Active Device and Capacitor Metallizations Within an Optimized Bond Envelope

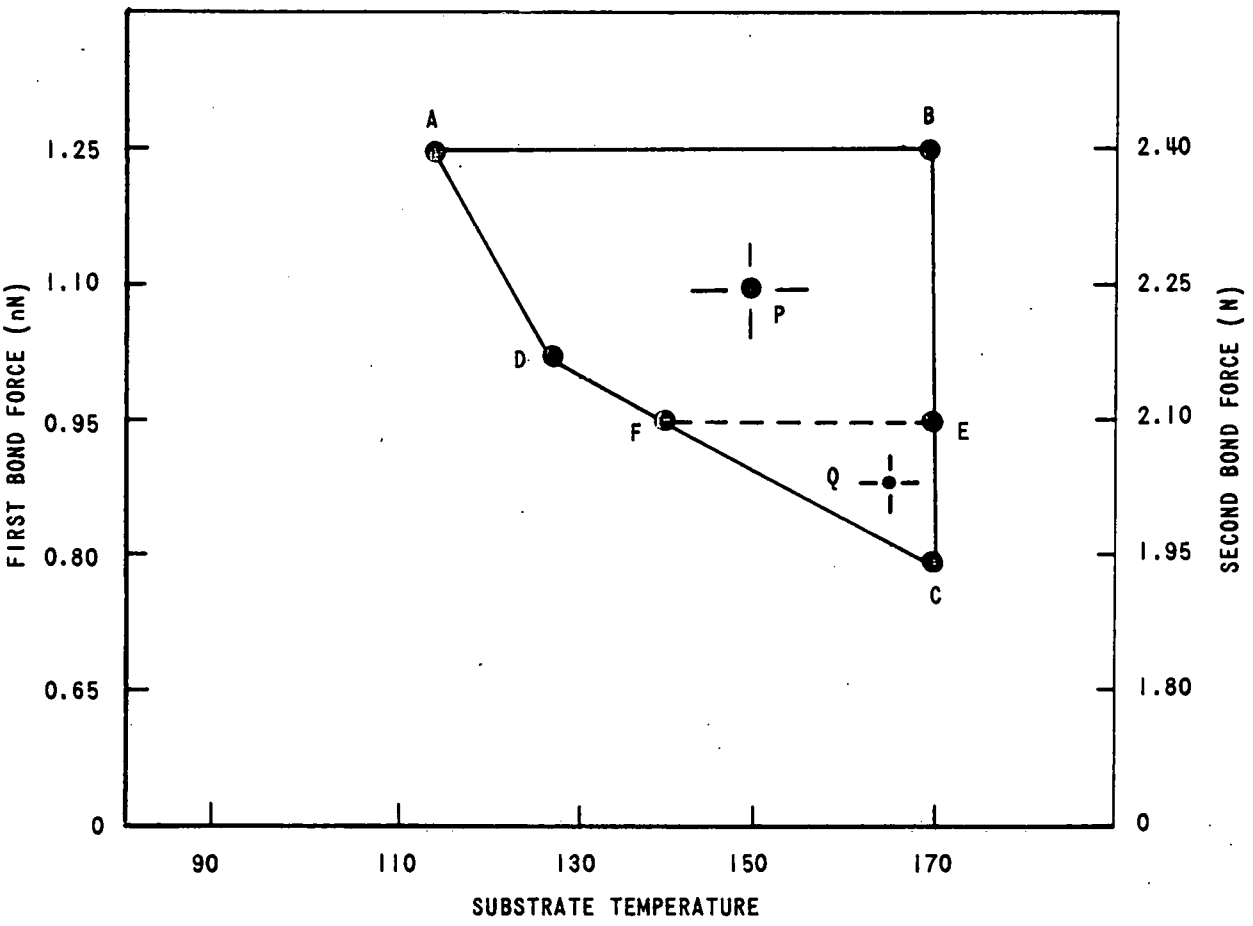

AB - SANDIA/BENDIX SUBSTRATE CONSTRAINT
BC - EPOXY CONSTRAINT
CD - CAPACITOR CONSTRAINT
DA - DEVICE CONSTRAINT
EF - VENDOR SUBSTRATE CONSTRAINT
P - OPTIMUM POINT, SANDIA/BENDIX
Q - OPTIMUM POINT, VENDOR

Figure 50. 1-Mil Bond Envelope

Bonding to capacitor metallization has been the less repeatable of TC wire bonding.[20] The chip capacitors used in the present study had thick film gold terminations. They were applied to the capacitor body by dipping the capacitor into a thick film paste and then firing the paste at 800 - 1000°C. The fired paste has a glassy phase at the surface which impedes TC bonding and varies the results. Bondability of chip capacitors varied from lot-to-lot. Some lots exhibited improved bondability when the bonding region was scratched or abraded with a soft eraser. The eraser

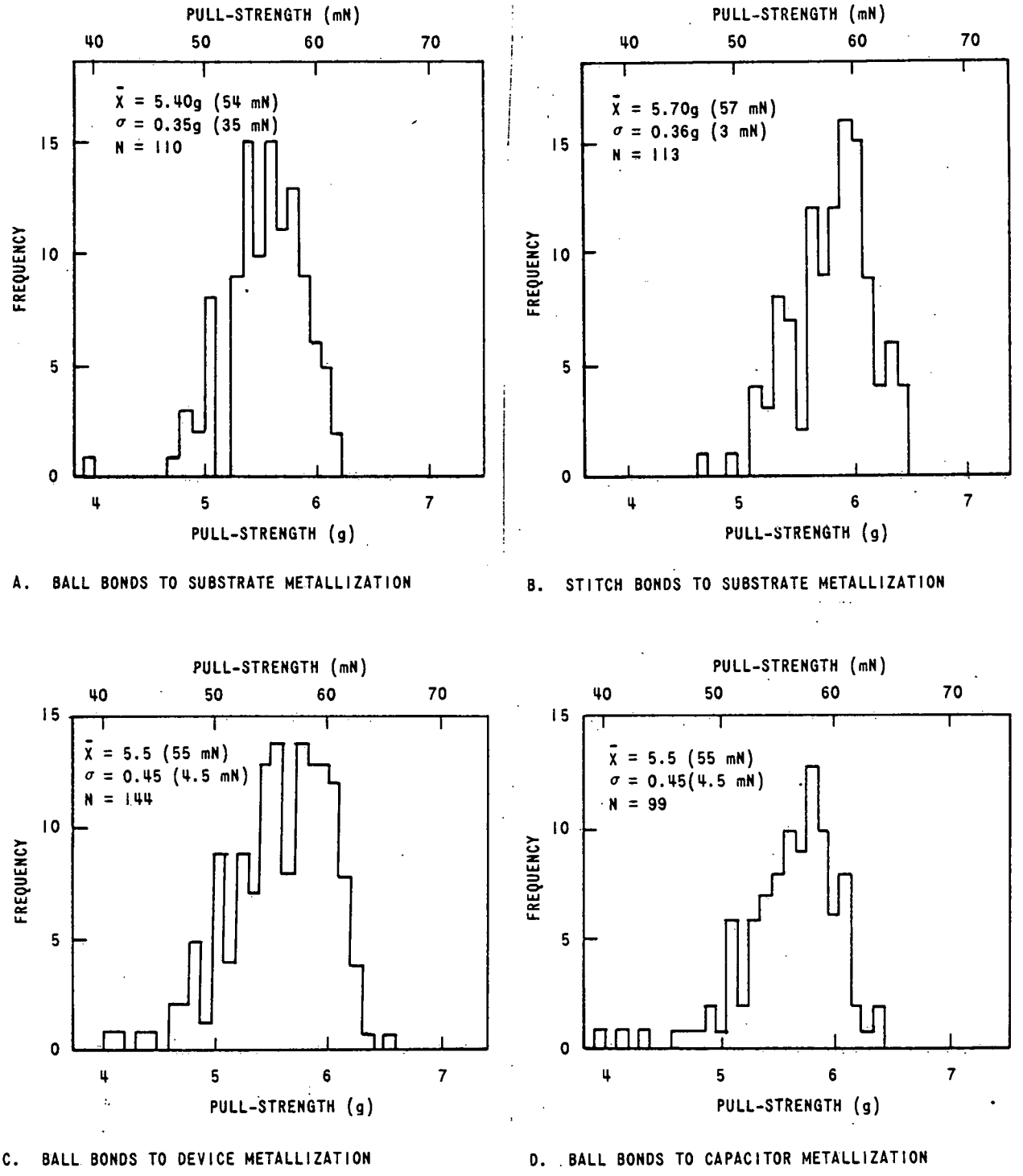

Figure 51. Optimized Pull Data on 1-Mil Wire

removed organic contamination. Additional work is needed to characterize thick film metallizations to improve TC bonding.[21]

Rework

Fine wire bonds can be removed with the same tool used to remove beam lead bonds. To determine the number of times a wire bond can be reworked without significantly degrading bond strength, four samples of ball bonds and four of stitch bonds were made and destructively pull tested. Following the first bond, the samples were reworked once, twice, or three times (Figures 52 and 53). In all cases the test failures were wire failures. Neither the mean nor minimum strength decreases significantly as the number of times the bond is reworked increased. A wire bond, therefore, can be reworked three times by scraping off the old bond and rebonding in the same location.

ACCOMPLISHMENTS

Beam lead devices were Wobble-tool bonded to chromium-gold thin films. The K & S Model 576 bonders were used. Bonding force and interface temperatures were characterized interface temperature was shown to be the linear combination of bonding tool temperature and substrate temperature. A characterization method was defined which allowed bonding parameters developed on one machine to be applied to similar machines. A study of beam lead cleanliness before bonding indicated that some vendor's BLDs need cleaning before bonding. The hardness of the beams could not be used as a beam qualification criteria. Plating conditions for the beams had to be controlled and the bondability of each plating lot had to be evaluated. Substrate metallization had to be etched before bonding to remove chromium oxide contaminants which formed during the 300°C, 2 hour resistor stabilization process.

Analysis of nondestructive and destructive test data showed that the following conditions maximized the mechanical integrity of the bonded devices.

- The mean device pull-off strength was greater than 1 gram per mil of (0.38 N/mm) of beam width, regardless of the failure mode.
- The number of bond delamination failures was less than 0.3 percent of the total bonds tested.
- The relative number of bond heel failures was not greater than 25 percent.

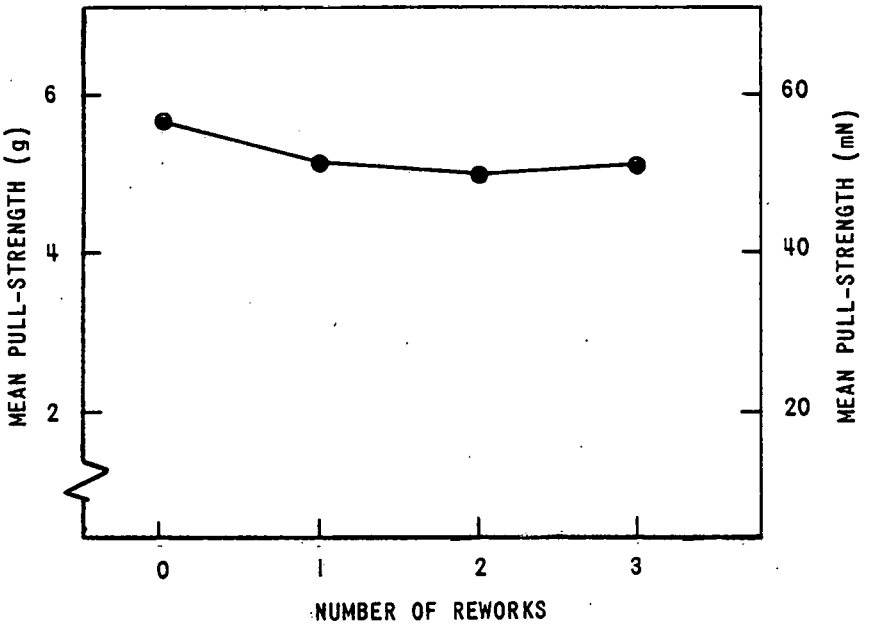

A. AVERAGE PULL-STRENGTH

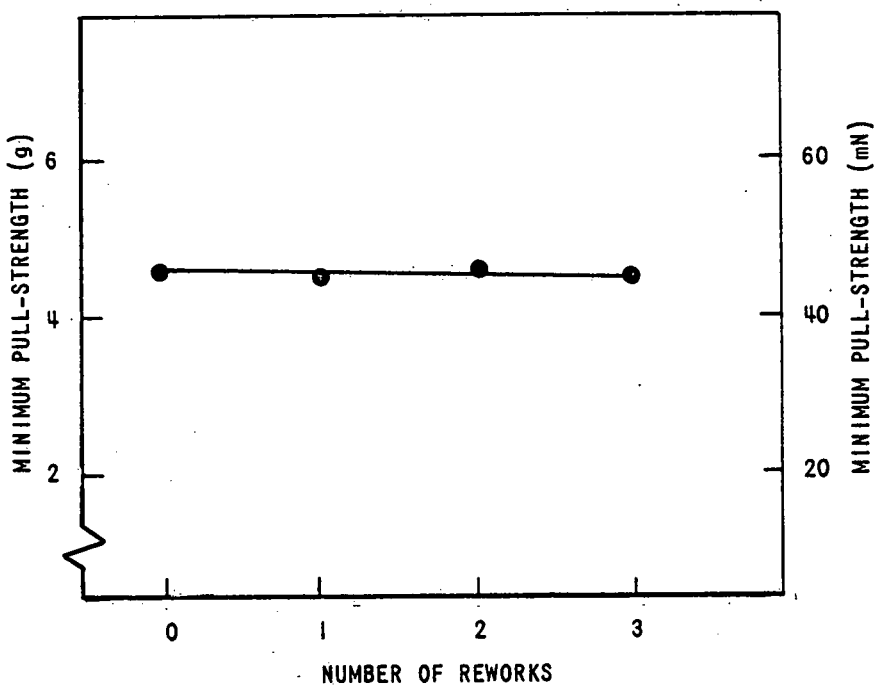

B. MINIMUM PULL-STRENGTH

Figure 52. Repair of 1-Mil Stitch Bonds

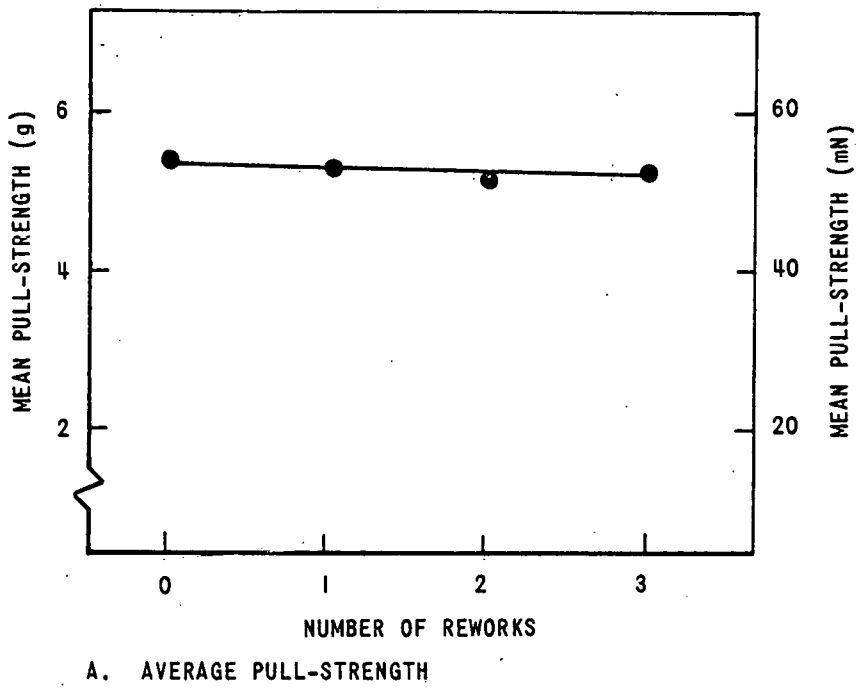

A. AVERAGE PULL-STRENGTH

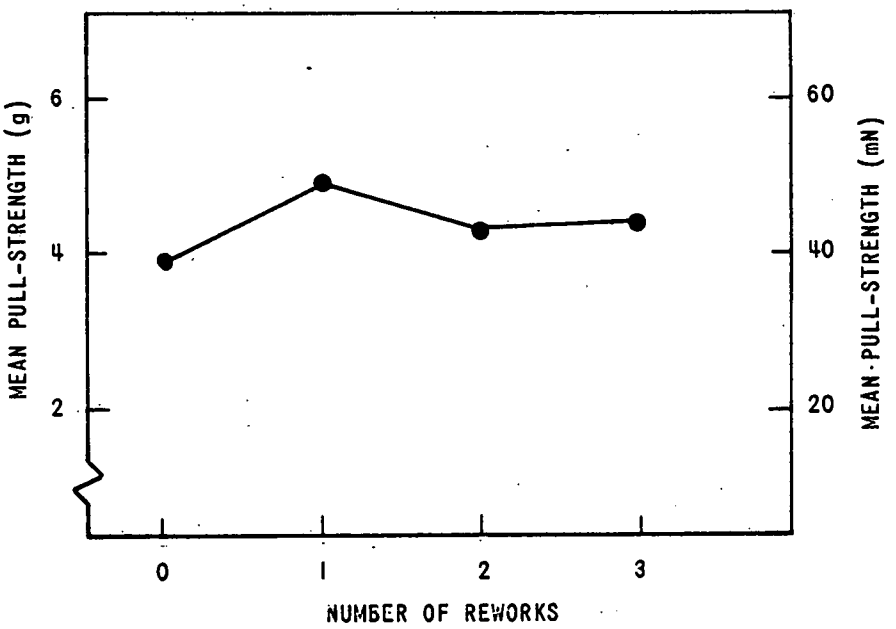

B. MINIMUM PULL-STRENGTH

Figure 53. Repair of 1-Mil Ball Bonds

The straightforward extrapolation of bonding schedule for four beam devices to larger format devices was not possible. Deformation on the corner beams is greater than the deformation of the center beam. A table was made to show the proper compensation of four beam bonding schedules that allowed extrapolation for larger format devices.

Beam lead bonds were scraped off and rebonded twice with no degradation in bond strength.

Thermocompression gold wire bonding was also characterized. Elongation of 0.003 inch (76 μm) wire was not a process variable, because the bonding operation caused the wire to reach a dead soft state. The bonder was set up to produce balls less than five wire diameters in size after flame off. Some reduction in bond strength would occur with balls larger than five wire diameters. It was difficult, however, to determine nondestructively when a ball had been excessively deformed. Flame-off tip orifice size, wire size, wire tension, the cutting speed of the flame, the thermal characteristics of the flame distance from the wire, and the bonding tool affected ball size.

A bond envelope was defined for the following combinations of metallization: gold bonding pads on HMCs, chip capacitor terminations, and chip-on-tab device metallization. Bondability of chip capacitors varied from lot-to-lot. Rework of fine wires could be done with the same tool used for beam lead rework. A wire bond could be reworked three times without affecting mean or minimum bond strength.

Beam lead wire TC bonding processes have been defined and transferred to HMC production at Bendix Kansas City.

FUTURE WORK

Four areas are recommended for future work.

- Bonding variability of chip capacitor terminations must be eliminated.
- Removal techniques of the BLD must preserve the device for postmortem analysis.
- Bonding methods for large format devices must develop a larger bond envelope.
- Nondestructive test methods for beam lead bonds must detect potentially weak bonds, cracked silicon nitride passivation layer, and cracked die.

REFERENCES

[1]F. L. English and others, *A Microcircuit Technology Development Program.* Albuquerque: Sandia Laboratories, Report SC-DR-70-514, July, 1970.

[2]Art Laudel, *Microelectronics Residency Support.* Bendix Kansas City: Report BDX-613-1265, December, 1974.

[3]T. S. Ellington, *Lead Frame Bonding.* Washington: Proceedings, 22nd Conference of Electronic Components, May, 1972, pp 357-361.

[4]*A Seminar on Beam Lead Technology.* Phoenix: Motorola's Beam Lead Laboratory, November 16, 1970.

[5]M. Byar, *Principles of Beam Lead Bonding.* Fort Washington, Pennsylvania: K and S Beam Lead Advanced Packaging Seminar, 1969.

[6]*Model 576 Beam Lead Bonder Operation Manual.* Fort Washington, Pennsylvania: Kulicke and Soffa Industries, 1971.

[7]J. R. Adams and H. Bonham, "Analysis and Development of a Thermocompression Bond Schedule for Beam Lead Bonding," *IEEE Transactions on Parts, Hybrids, and Packaging,* Volume PHP-8, Number 3, September, 1972, pp 22-26.

[8]F. L. Howland, *Beam Lead and Wire Thermocompression Bonding.* Washington: Proceedings, 21st Conference of IEEE Electronic Components, May, 1971, pp 285-288.

[9]C. D. Henning and R. Parker, "Transient Response of an Intrinsic Thermocouple," *Journal of Heat Transfer,* May, 1967, p 146.

[10]J. R. Adams and H. L. Floyd, *Evaluation of the Mechanical Integrity of Beam Lead Devices and Bonds Using Thermomechanical Stress Waves.* Las Vegas: Proceedings, 9th Annual Symposium of Reliability Physics (IEEE), 1971, pp 187-194.

[11]N. T. Panousis and H. Bonham, *Bonding Degradation in the Tantalum-Nitride-Chromium-Gold Metallization System.* Las Vegas: Proceedings of the 11th Annual Symposium of Reliability Physics, 1973, pp 21-25.

[12]P. S. Kenrick, *Nature.* Volume 217, 1968, p 1249.

[13]J. R. Rairden, C. A. Neugebauer, and R. A. Sigsbee, *Metallurgical Transactions.* Volume 2, Issue 3, 1971, p 719.

[14]J. K. Hirvonen, W. H. Weisenberger, J. E. Westmoreland, and R. A. Meussner, *Applied Physics Letter*. Volume 21, Number 1, 1972, p 37.

[15]R. E. Thomas and G. A. Haas, *Journal of Applied Physics*. Volume 43, Number 12, 1972, p 4900.

[16]W. R. Berry, P. M. Hall, and M. T. Harris, *Thin Film Technology*. Princeton: D. Van Nostrand Company, 1968.

[17]"How to Lower Cost of Semiconductor Assembly with High Quality Lead Bonding Wire," *Circuits Manufacturing*. December, 1971, pp 41-42.

[18]P. H. Holloway and R. L. Long, Jr., *Evaluation of Prebond Etchants in Hybrid Microcircuit Processing*. Albuquerque: Sandia Laboratories, Report SLA-73-1049, March, 1974.

[19]C. M. Tapp and D. J. Sharp, *A Compilation of Specifications Describing Hybrid Microcircuit Technology*. Albuquerque: Sandia Laboratories, Report SLA-74-0300, June, 1974.

[20]D. W. Bushmire, *Capacitor Bonds in the MC2305 Hybrid Circuit*. Albuquerque: Sandia Laboratories, Report SC-DR-72005, September, 1972.

[21]E. L. Chavez, *Thermocompression Bonding Capabilities of Metallized Termination on Discrete Components*. Albuquerque: Sandia Laboratories, Report SLA-73-0835, December, 1973.

DISTRIBUTION

	Copy
R. Bulcock, ERDA-KCAO	1
V. C. Vespe, ERDA-KCAO	2
J. R. Adams, SLA	3
D. W. Bushmire, SLA	4
A. R. Engquist, SLA	5
J. T. Grissom, SLA	6
D. R. Johnson, SLA	7
G. W. Rodgers, SLA	8
C. M. Tapp, SLA	9
R. K. Traeger, SLA	10-11
R. F. Pippert, D/100	12
D. J. Stevens, D/141	13
J. D. Corey, D/554	14-15
L. Stratton, D/554	16-17
R. P. Frohmberg, D/800	18
D. H. Hax, D/800	19
F. A. Spies, D/800	20
B. T. Lampe, D/814	21
A. O. Bendure, D/842	22-24
B. W. Lenhardt, D/842	25
J. O. Losure, D/842	26
J. A. Peters, D/842	27
D. D. Peterson, D/842	28
W. A. Piper, D/842	29
L. E. Schantz, D/842	30
T. A. Wiley, D/842	31
D. L. Willyard, D/842	32
D. A. Youngberg, D/842	33
L. W. Siever, D/863	34
L. W. Smith, D/863	35
J. H. Swafford, D/863	36
R. E. Kessler, D/864	37